

# **2 In plane loading – walls and beams**

## **2.1 Stress fields**

## Learning objectives

Within this chapter, the students are able to:

- create simplified stress fields and strut-and-tie models for walls, beams and frames, including discontinuity regions, as a combination of basic stress fields and strut-and-tie models.
  - discuss the differences and similitudes between stress fields and strut-and-tie models.
  - identify the critical regions of a simplified stress field or strut-and-tie model and formulate detailed stress fields allowing for the verification of those regions.
  - verify most frequent nodal zones.
- assess the applicability of stress fields and strut-and-tie models, particularly concerning (i) the presence of transversal reinforcement, (ii) the selection of suitable effective compressive strength, (iii) the proper detailing of nodal zones and (iv) the existence of relevant 3D effects. Whenever 3D effects are present, the students are able to create 2D stress fields and strut-and-tie models capturing those effects.

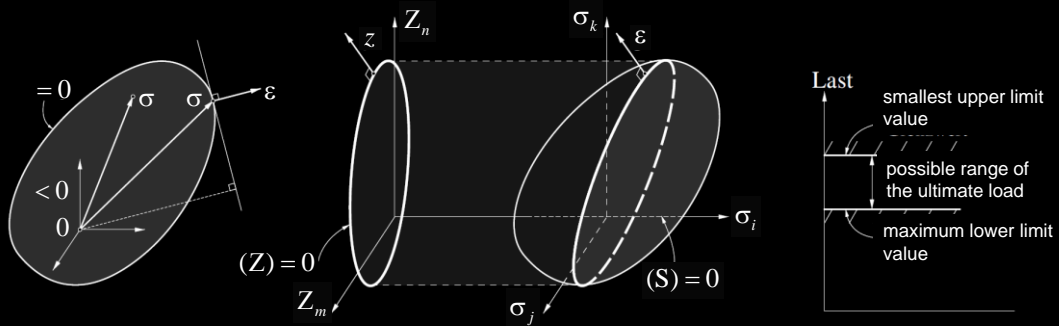
# Stress fields

## Strut-and-tie models and stress fields: Historical development

- Originally, solutions followed primarily the main load path, the dimensions of the struts being of second importance. Such models have persisted until today («Strut-and-tie models», e.g. Schlaich et al., 1984 and 1987).
- Since about 1975, strut-and-tie models (truss models) have been used in combination with the assumption of a **limited concrete compressive strength  $f_c$** . The dimensions of the struts and nodal zones result from the assumption of  $f_c$ .
- The resulting strut-and-tie models (truss models) are **statically admissible (discontinuous) stress fields** according to the **lower bound (static) theorem of the theory of plasticity** and, therefore, are based on a consistent theoretical basis.
- Computer-aided methods for the development of stress fields have been developed at various universities (e.g. the Compatibility Stress Field Method, CSFM, developed at ETH Zürich in collaboration with the company IDEA StatiCa). The use of these methods is starting to become more common in practice. These methods will be discussed in the chapter about numerical modelling.

The lectures “Stahlbeton I” and “Stahlbeton II” have already dealt with stress fields; the topic is repeated and deepened in this lecture.

## Stress fields



- The application of stress fields is based on the **theory of plasticity**.
- ETH Zurich played a central role in their development - namely Professors Bruno Thürlimann and Peter Marti.
- Internationally this approach is known as the "Zurich School". It is based on consistent mechanical models, which are verified with large-scale tests.

Like many other design methods, the application of stress fields in reinforced concrete design is based on the theory of plasticity (implicitly or explicitly).

ETH Zurich's Prof. Bruno Thürlimann and his successor Prof. Peter Marti were pioneers in the application of plasticity theory to reinforced concrete, see "Stahlbeton I" (Introduction).

Limit analysis theorems of plasticity:

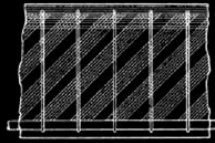
- *Lower bound theorem of limit analysis*: Every loading for which it is possible to specify a statically admissible stress state that does not infringe the yield condition is not greater than the ultimate load.
- *Upper bound theorem*: Every loading that results from equating the work of external forces for a kinematically admissible deformation state with the associated dissipation work is not less than the limit load.
- *Compatibility theorem*: Verification of the previous two.

## Stress fields

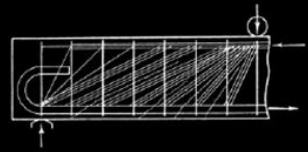
### Early truss models (descriptive)



K. W. Ritter, «Die Bauweise Hennebique» (1899)

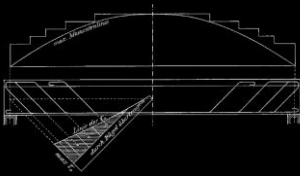


E. Mörsch, «Der Eisenbetonbau» (1908)

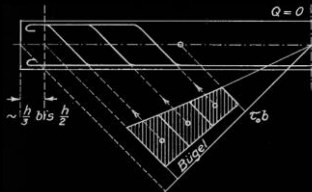


E. Mörsch, «Der Eisenbetonbau» (1922)

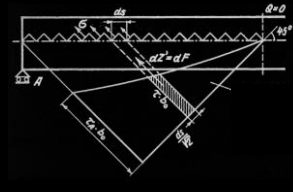
### Elastic stress fields with principal tensile stresses (semi-empirical)



E. Mörsch, «Der Eisenbetonbau» (1908)



M. Ritter, «Vorlesung Massivbau» (ca. 1940)



P. Lardy, «Vorlesung Massivbau» (1951)

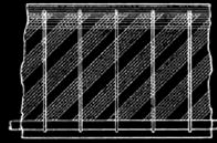
Even though sometimes presented this way, truss models have not been used for dimensioning concrete structures for more than 100 years. Ritter and Mörsch already explained the load-bearing behaviour using these models, but these were not dimensioning tools. Until the 1960s these "simple" models were used by outstanding engineers, but rather "in a hiding way" since they were not considered scientific. From the beginning of concrete construction up to the 1960s the design was officially carried out using elastic stress fields (for example with diagonal principal tensile stresses, see figures) and comparing to some admissible stresses.

# Stress fields

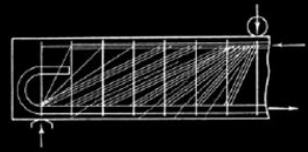
Early truss models (descriptive)



K. W. Ritter, «Die Bauweise Hennebique» (1899)

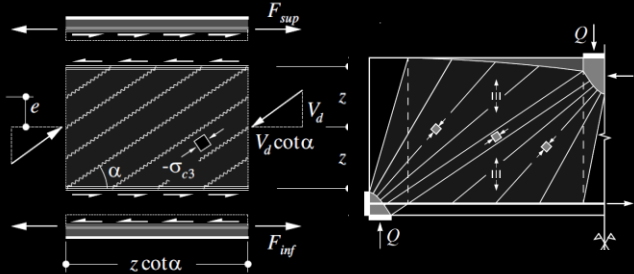
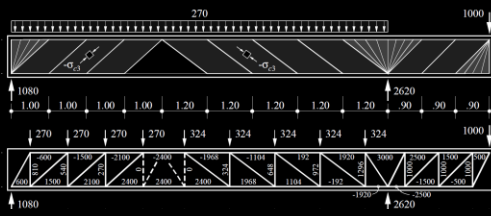


E. Mörsch, «Der Eisenbetonbau» (1908)



E. Mörsch, «Der Eisenbetonbau» (1922)

Current strut-and-tie models / Stress fields: **theory of plasticity = consistent foundation**



## Structural concrete at the ETH - former professors



Karl Culmann  
1821-1881  
Prof. 1855-1881  
(→ Ritter)



Karl Wilhelm Ritter  
1847-1906



Emil Mörsch  
1872-1950



Arthur Rohn  
1878-1956



Max Ritter  
1884-1946

### Pioneers in the application of the theory of plasticity to structural concrete members



Pierre Lardy  
1903-1958  
Prof. 1946-1958  
(→ Thürlimann)



Bruno Thürlimann  
1923-2008  
Prof. 1960-1990  
(→ Marti)



Hugo Bachmann  
1935  
Prof. 1969-2000  
(→ Stojadinovic)

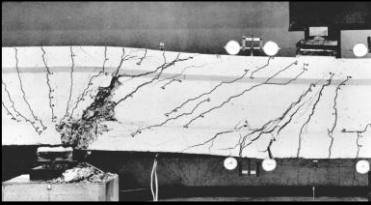


Christian Menn  
1927-2018  
Prof. 1971-1992  
(→ Vogel)

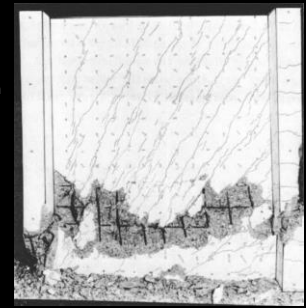


Peter Marti  
1949  
Prof. 1990-2014  
(→ Kaufmann)

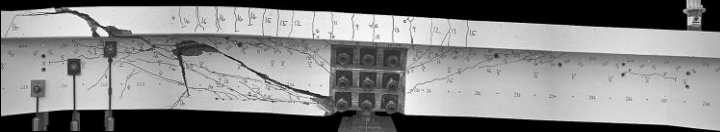
## Plastic design methods



Bachmann / Thürlimann  
(1965)



Maier / Thürlimann  
(1985)

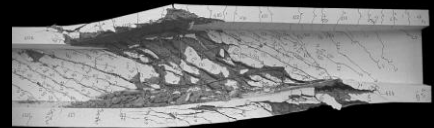


Stoffel / Marti  
(1995)



Sigrist / Marti  
(1992)

Kaufmann / Marti  
(1995)



Examples of large-scale experiments carried out at ETH Zurich to validate mechanically consistent models.



## Stress fields

### Principles for the design of stress fields

There are usually several suitable stress fields to solve the same problem. Designers select the most suitable stress field and dimension the reinforcement accordingly.

The consideration of the following principles usually ensures an economic design (the requirement for stiffness also follows from the principle of the minimum complementary energy):

- **Simplicity** (usually only orthogonal reinforcement is used)
- **Stiffness** (e.g. short ties)
- **Efficiency** (consider minimum reinforcement in the calculation)

A scaled drawing of the model is highly recommended.

In any case, sufficient minimum reinforcement should be used ( $\rho = 0.1\text{...}0.3\%$ , depending on the region).

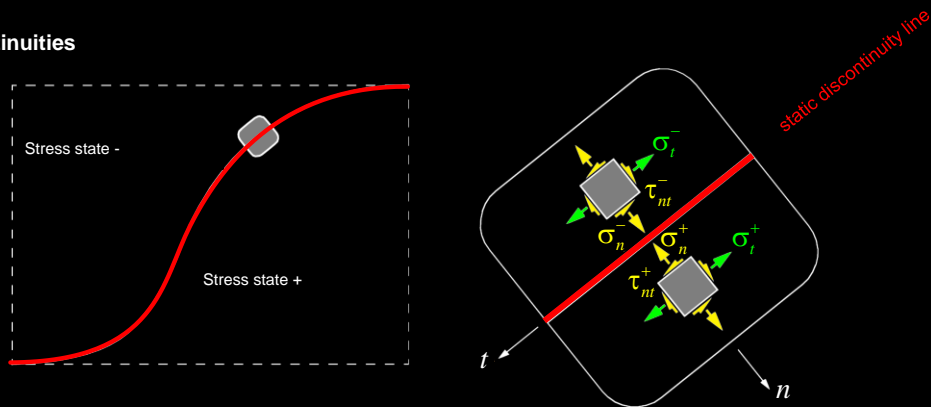
Particular attention should be paid to the choice of the effective concrete compressive strength, that should account for the non ideally plastic behaviour of concrete (see separate chapter) and has a decisive influence on the geometry of the model.

By using stress fields, both the multidimensional load-bearing behaviour of concrete and the contribution of distributed reinforcement layers can be considered with any desired level of approximation.

Plane discontinuous stress fields are suitable for practical applications and are composed of several individual basic elements connected through discontinuities. These models are formed by a group of principal stress trajectories subjected to uniaxial or biaxial stresses (in the case of nodal regions with biaxial uniform compressive stress states, often inaccurately referred to as "hydrostatic", the group of stress trajectories degenerates). These trajectories can be parallel to each other (struts and ties) or divergent (fans and arches).

# Stress fields

## Stress discontinuities



Lower bound theorem of the theory of plasticity: equilibrium must be fulfilled

→ Normal stresses parallel to the discontinuity line may have a discontinuity ( $\sigma_t^- \neq \sigma_t^+$  is admissible)

→ Normal stresses perpendicular to the discontinuity line and shear stresses must be continuous ( $\sigma_n^- = \sigma_n^+$  and  $\tau_{nt}^- = \tau_{nt}^+$  must be fulfilled)

## Repetition Stahlbeton I:

Discontinuous stress fields have statically admissible stress discontinuities where the equilibrium conditions shown in the figure must be fulfilled.

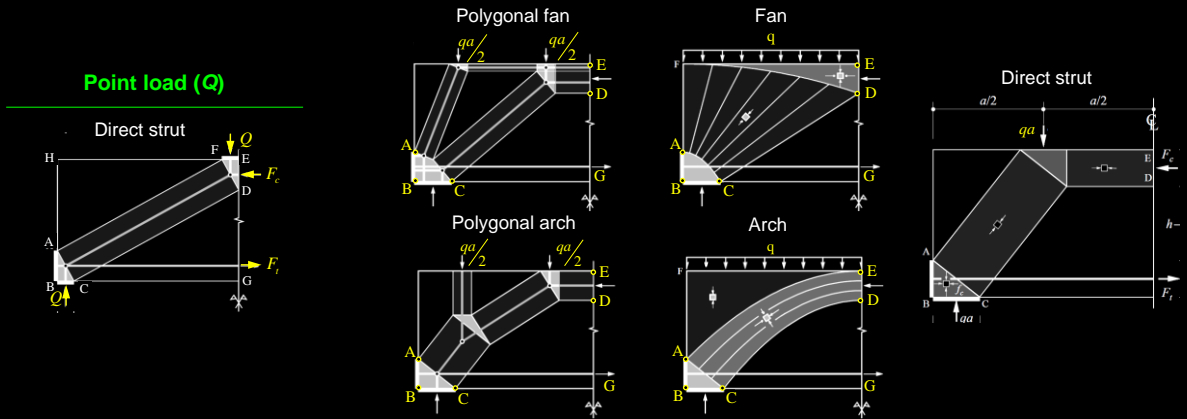
Strut-and-tie models are simple discontinuous stress fields: a compressive stress field acts in the strut and parallel to it, while immediately adjacent to the strut the stress is zero. These models make it possible to formulate a statically admissible equilibrium state for any structural element and loading configuration and allow visualizing one (among many possible) admissible force flow in the structure.

# Stress fields

## Basic models for beams

(a) without transverse reinforcement

Distributed load ( $q$ )



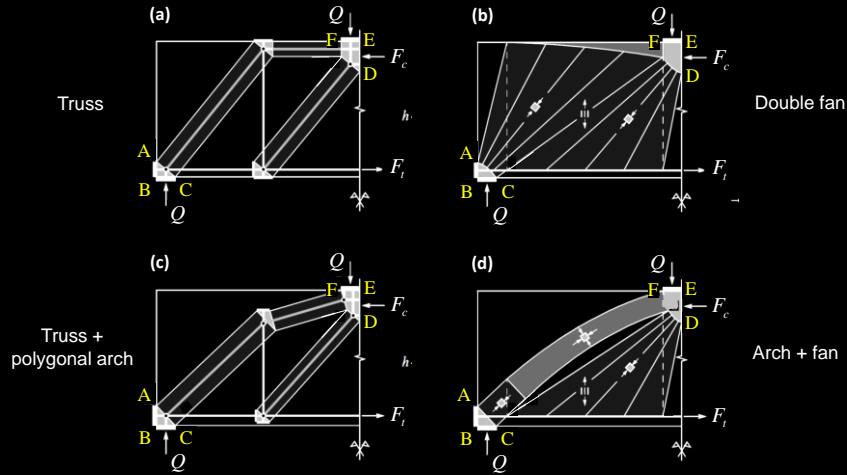
## Basic models for beams:

The slide shows an overview of possible stress fields in **beams without transversal reinforcement**. A distributed load can be model in different ways: continuously (which leads to a fan or arch stress field), as two equivalent point loads (which leads to a polygonal fan or arch) or as one equivalent point load (which leads to a direct strut mechanism). The resultant reinforcement, positions of points A to E and the predicted lower bound of the ultimate load are identical in all cases.

# Stress fields

## Basic models for beams

(b) with transverse reinforcement and point load ( $Q$ )



## Basic models for beams:

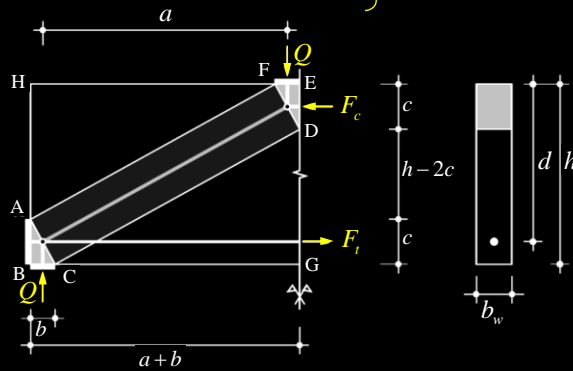
The slide shows an overview of basic stress fields in **beams with transversal reinforcement**. Instead of transferring the load directly to the support via compression elements, it can be partially (arch mechanisms) or totally suspended by placing vertical (shear) reinforcement.

## Stress fields

### Derivation of direct strut mechanism (point load + no transverse reinforcement)

Equilibrium:

$$\left. \begin{aligned} F_c = b_w c f_c = A_s f_{sy} = F_t \\ Qa = b_w c f_c (h - c) \end{aligned} \right\} \begin{aligned} c = \frac{h}{2} - \sqrt{\frac{h^2}{4} - \frac{Qa}{b_w f_c}} \\ A_s = b_w c \frac{f_c}{f_{sy}} \end{aligned} \left. \begin{aligned} \rho = A_s / (b_w d) \\ \omega = \rho (f_{sy} / f_c) \end{aligned} \right\} \begin{aligned} Q = \frac{b_w f_c h^2}{a} \cdot \frac{\omega(1-\omega/2)}{(1+\omega/2)^2} \quad \left( \omega \leq \frac{2}{3} \right) \\ Q = \frac{b_w f_c h^2}{4a} \quad \left( \omega \geq \frac{2}{3} \right) \end{aligned}$$



$$\begin{aligned} b &= \frac{Q}{b_w f_c} \\ c &= \omega d, \quad \omega = \frac{A_s f_{sy}}{b_w d f_c} \\ F_c = F_t &= \omega d b_w f_c \end{aligned}$$

22.09.2021

ETH Zurich | Chair of Concrete Structures and Bridge Design | Advanced Structural Concrete

13

### Direct strut mechanism

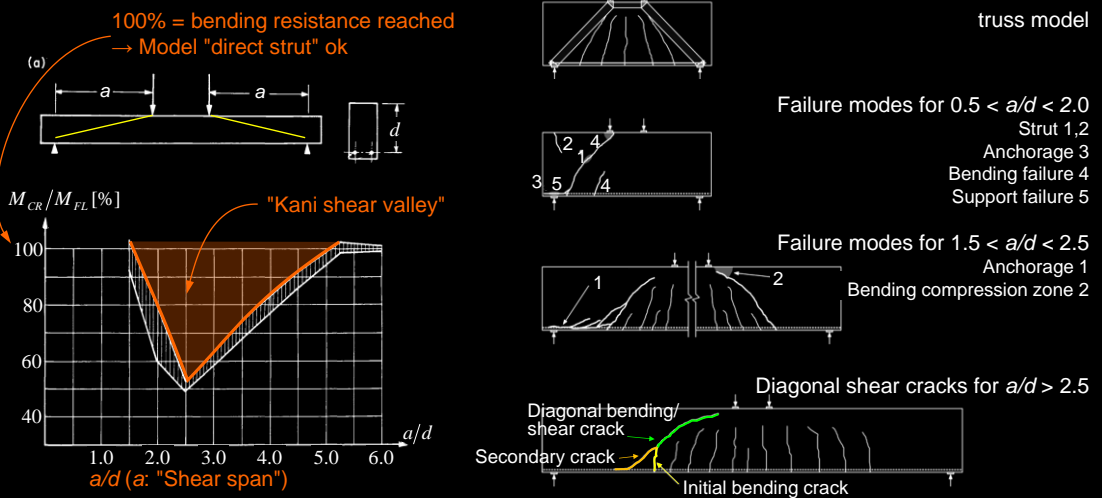
The figure shows one half of a symmetrical beam element with a rectangular cross section, without vertical reinforcement and with a single applied vertical load  $Q$ . The load is transferred directly to the support via the concrete strut  $ACDF$ , which is in equilibrium with the reaction force and the force  $F_t$  acting in the horizontal tie. The introduction and deviation of the load and the reaction require the nodal zones  $ABC$  and  $DEF$ . The dimensions of the supports and the anchor plates, which define the dimensions of the nodal zones, depend on the verification of the concrete compressive strength at their edges. Therefore, the nodal zones are subjected to a biaxial, uniform compressive stress state ( $\sigma_{c1} = \sigma_{c3} = -f_c$ ). The strut consists of parallel stress trajectories subjected to uniaxial compression with  $-f_c$ .

The selected equilibrium model is called "direct strut" and is a rough idealization of the load-bearing behaviour. The model does not require a vertical tie; therefore, the force in the horizontal tie  $F_t$  occurring in the middle of the member must be completely anchored behind the support. In the areas  $CGD$  and  $AFH$ , the concrete is stress-free.

# Stress fields

## Limits of applicability of direct strut model

G.N.J. Kani ("The Riddle of Shear Failure and its Solution", 1964): Results of experiments without stirrups



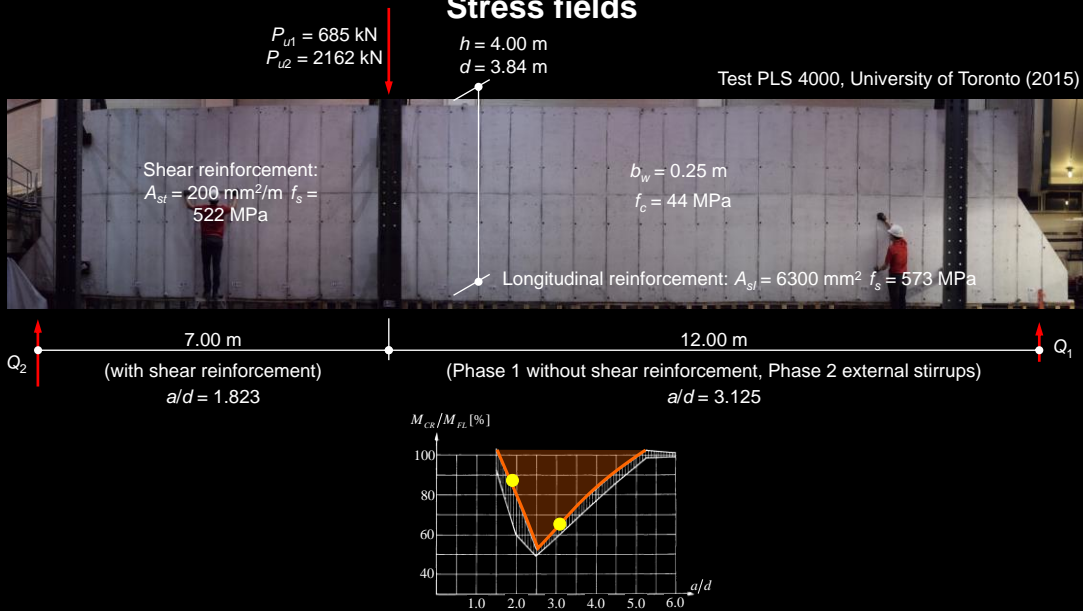
## Is the direct strut generally applicable?

The theory of plasticity cannot be generally applied in elements without a minimum amount of transversal reinforcement, even if a statically admissible stress state can be found. The reinforcement should avoid brittle failures. The best-known examples of brittle failures are "shear tests" on beams without shear reinforcement (three-point or four-point bending tests). These experiments have little in common with real structures because (i) simple supported beams with concentrated loads are rare in practice and (ii) the size of the experiments is typically much smaller than the size of real structural members. In spite of these limitations many of these experiments have been conducted in the past, and even nowadays new shear tests are performed.

In experiments with a "shear slenderness" ( $a/d$ , shear span to effective depth ratio) in the range of 2.5 to 3.5, a brittle failure is triggered by a diagonal shear crack, which often forms from an existing bending crack close to the support. For smaller and larger slenderness, the bending capacity (obtained e.g. according to a 'direct strut' stress field model) can be achieved. The critical zone for the shear slenderness was identified by G. N. J. Kani and is often called the "Kani shear valley".

Many material and structural properties modify the shape of the "Kani shear valley". For example, it should be noted that the ultimate load of beams reinforced with plain bars "without" (with very weak) bond is higher than the ultimate load of beams reinforced with ribbed bars (as soon as the anchorage is properly detailed, e.g. by using anchor plates). The most favourable case is the one of beams with pre-stressed unbonded longitudinal reinforcement (in this case just one bending crack at midspan tends to occur). The presence of shear reinforcement, reduces or even eliminates the "Kani shear valley".

## Stress fields



### Is the direct strut generally applicable? Experimental test example

A blind prediction was conducted by Collins, Bentz and Quach at the University of Toronto to estimate the ultimate load in a very large shear test (beam height 4 m). A beam with a height of only 30 cm was tested simultaneously in order to demonstrate the influence of the beam height on the shear capacity (so-called "size effect"). This large scale experiment impressively demonstrates the decisive mode of failure.

The left span was reinforced with stirrups in order to ensure that the failure occurs in the long span (without stirrups).

## Stress fields



22.09.2021

ETH Zurich | Chair of Concrete Structures and Bridge Design | Advanced Structural Concrete

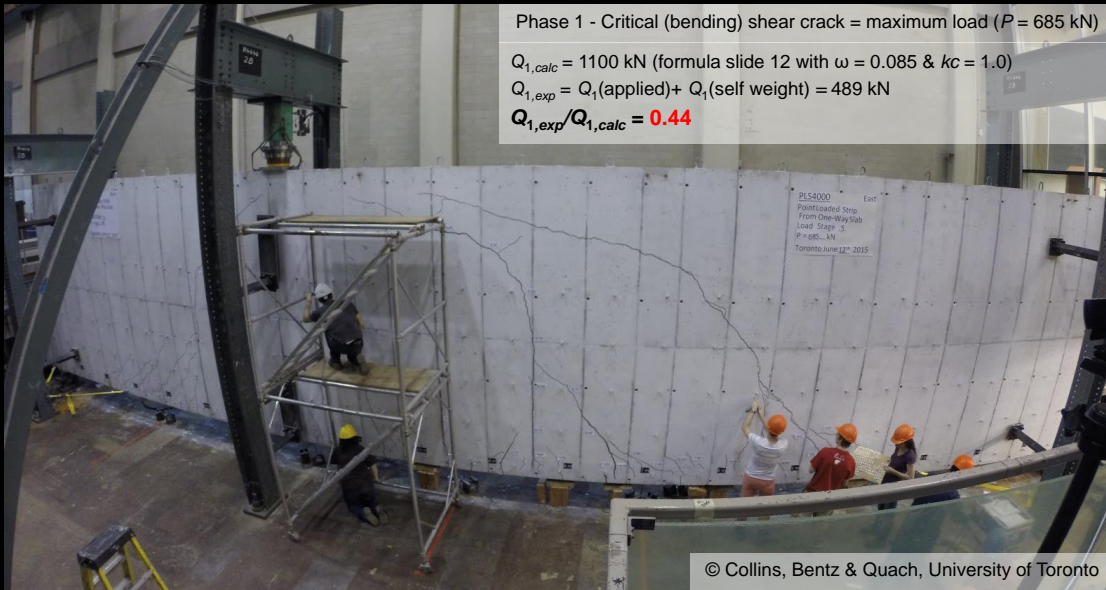
16

### Is the direct strut generally applicable? Experimental test example

The image shows bending cracks, and bending-shear cracks originating from the bending cracks, with increasing inclination.



## Stress fields



22.09.2021

ETH Zurich | Chair of Concrete Structures and Bridge Design | Advanced Structural Concrete

17

### Is the direct strut generally applicable? Experimental test example

The typical failure mode at this  $a/d$  ratio is certainly different to the «cross-sectional verification» specified by codes. As seen in the picture, the critical shear crack in the experiment originated from a bending crack close to the support (area with large  $V$ , but rather small  $M$ , i.e. large gradient for bond).

The nominal ultimate shear stress in the nominal design section at a distance of  $d/2$  from the right-hand support, which is the verification section according to SIA 262, was about 0.46 MPa, taking into account the dead weight (i.e. about 0.30 MPa would have been "safe" for design).

Prediction of the capacity with a direct strut mechanism (assuming a concrete reduction factor  $k_c = 1.0$  corresponding to an undisturbed uniaxial compressive stress state) would lead to a large overestimation of the ultimate load:

- $Q_{1,calc} = 1100 \text{ kN}$  (according to formula slide 12 with  $\omega = 0.085$ )
- $Q_{1,exp} = Q_1(\text{applied}) + Q_1(\text{self weight}) = P_{U1} \cdot (7 \text{ m} / 19 \text{ m}) + 0.25 \text{ m} \cdot 4 \text{ m} \cdot 25 \text{ kN/m}^3 \cdot 19 \text{ m} / 2 = 489 \text{ kN}$
- $Q_{1,exp}/Q_{1,calc} = 0.44$

## Stress fields



22.09.2021

ETH Zurich | Chair of Concrete Structures and Bridge Design | Advanced Structural Concrete

18

### Is the direct strut generally applicable? Experimental test example

After failure occurred, the beam was reloaded because some participants in the blind prediction competition complained that the beam still had not failed. However, the previous ultimate load could not be reached anymore (but the shear crack became more visible).

## Stress fields



22.09.2021

ETH Zurich | Chair of Concrete Structures and Bridge Design | Advanced Structural Concrete

19

### Is the direct strut generally applicable? Experimental test example

The large span was then reinforced with external reinforcement such that it has a much higher shear reinforcement amount than the short span. The load was applied again.

## Stress fields



22.09.2021

ETH Zurich | Chair of Concrete Structures and Bridge Design | Advanced Structural Concrete

20

The failure in phase 2 (with transverse reinforcement) was much more ductile. The cracks can be observed forming a fan, as required to activate the distributed shear reinforcement (load suspension mechanism, see following slides). Based on the developed cracks, it seems that the load-bearing mechanism corresponds to the double fan mechanism presented on slide 11, which will be further discussed in the following.

In a section at a distance  $z$  from the left support, the nominal shear stress at failure, taking the permanent loads into account, was about  $1.6 \text{ MPa}$ .

# Stress fields

## Limits of applicability of direct strut model

The presented **stress fields** for **beams without transverse reinforcement** are strong **simplifications** of reality:

- The **tension chord** is modelled like reinforcement without bond, but with an anchor plate that anchors the entire load. In reality, bond stresses lead to successive crack formation, and only for loads significantly higher than the cracking load a direct strut mechanism occurs.
- If no **minimum reinforcement** is placed in the member, there is the possibility that a diagonal crack penetrates into the compression field and the structure fails before the desired load-bearing mechanism is achieved. This is associated with a brittle failure (scale effect!).

The behaviour can be improved by **prestressing** the tension chord, which forces the direct strut mechanism.

In any case, a load transfer by a **direct strut mechanism** (without prestressing) is only meaningful in squat elements. In slender elements, the nodal zones' dimensions become very large and the anchorage of the reinforcement becomes problematic because the entire tensile force must be anchored behind the bearing!

These problems can be solved by providing **transverse reinforcement** (or by the activation of the vertical minimum reinforcement, which must **always** be placed).

## On the importance of minimum reinforcement:

In beams (and slabs) without shear reinforcement, the minimum vertical reinforcement is missing and brittle failures might occur. Therefore, the theory of plasticity cannot be applied in elements without a minimum amount of transversal reinforcement, even if a statically admissible stress state can be found (e.g. in the form of a direct strut mechanism modelled with strut-and-ties). Such models do not provide a safe estimation (lower bound) of the ultimate load if a brittle failure occurs earlier.

## Stress fields

**Fan and arch mechanisms: beams without transverse reinforcement & distributed load** (see also [4], p. 58ff)

The figure shows 4 possible models for the same problem. The formation of a fan or an arch mechanism depends, among other aspects, on:

- Slenderness of the element
- Amount of reinforcement
- Loading history

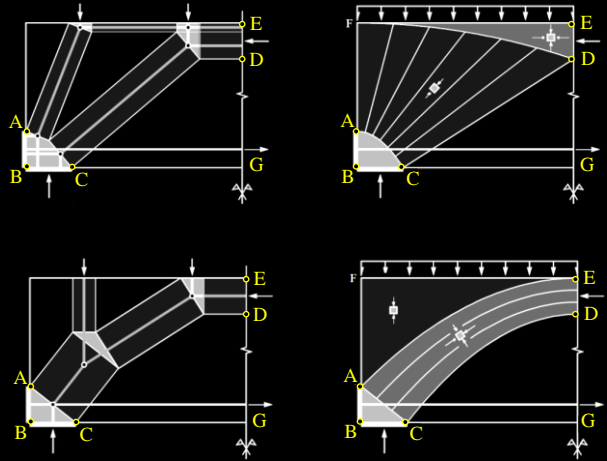
The strut geometry and the dimensions of the bearings are selected such that a biaxial compressive stress state is obtained in the nodal zone ABC in all examples:

$$\sigma_{e1} = \sigma_{e3} = -f_c$$

→ The location of **points A to E**, as well as the lower bound of the ultimate load, is identical in all models.

Note: Elastically the stiffer model tends to form (minimum complementary energy, i.e.

$$U^* = \int \varepsilon(\sigma) d\sigma \rightarrow \min$$



## Fans and arches in beams without transverse reinforcement

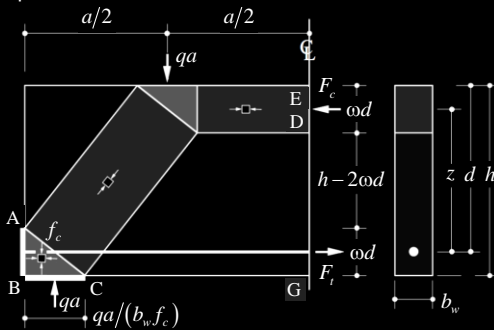
The figure illustrates the transition from simple strut-and-tie models to stress fields with non-parallel trajectories or to stress fields with variable compressive stresses along the trajectories. As in the previous slide, the beam element under consideration has only a longitudinal reinforcement. To ensure equilibrium, the loads must again be transferred directly to the support and the reinforcement force  $F_t$  in the tie at midspan must be fully anchored behind the support.

The basic case of a direct strut shown in the previous slide can be further developed to the two models on the left by considering two individual loads. By adding (infinitely many) further individual loads, the fan or arch mechanisms on the right can be derived, and serve to support a distributed load. Whether a fan or an arch mechanism occurs in a certain member depends, among other things, on the slenderness, the reinforcement ratio and the loading history. In an elastic solution the stiffest mechanisms will be formed (minimum complementary energy  $U^*$ , which corresponds to the deformation energy  $U$  for linear elastic behaviour).

In case the dimensions of the bearing and anchoring plates, as well as the geometry of the struts and the fan or arch, are selected such that a biaxially uniform compressive stress state ( $\sigma_{c1} = \sigma_{c3} = -f_c$ ) results in the nodal zones ABC, the location of points A to E is identical in all models.

## Stress fields

Since the location of points A...E is identical in all the models, the geometry can be defined from any of them, or even from a simpler model:



Geometric/mechanical reinforcement ratio:

$$\rho = \frac{A_s}{b_w d} \quad \omega = \rho \frac{f_y}{f_c} \quad h = d(1 + \omega/2)$$

Equilibrium:

$$\omega d b_w f_c d (1 - \omega/2) = \frac{q a^2}{2} \left( 1 - \frac{q}{b_w f_c} \right)$$

Solutions of the quadratic equation resulting from the equilibrium condition:

$$q = \frac{b_w f_c}{2} \left( 1 - \sqrt{1 - \frac{8h^2}{a^2} \cdot \frac{\omega(1-\omega/2)}{(1+\omega/2)^2}} \right) \quad \text{for } \omega \leq 2/3$$

$$q = \frac{b_w f_c}{2} \left( 1 - \sqrt{1 - \frac{2h^2}{a^2}} \right) \quad \text{for } \omega \geq 2/3$$

It is also possible to formulate a relationship for the mechanical reinforcement ratio required to resist a certain load  $q$  (see [4]).

## Fans and arches in beams without transverse reinforcement: Admissible load / required reinforcement

In all four models shown in the previous slide, the required mechanical reinforcement ratio is the same for a given load. For a given reinforcement ratio, the load  $q$  which can be supported is shown in this slide for all four models.

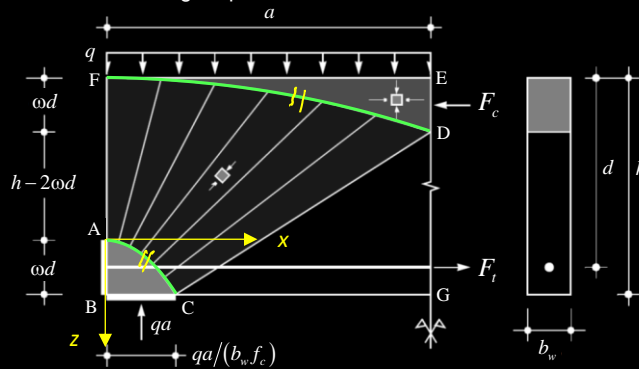
There are kinematically admissible failure mechanisms that are compatible with the presented models based on equilibrium (e.g. bending mechanisms with centre of rotation in D and one or more so-called collapse cracks in the CDG region). Therefore, the relationships given for  $q$  are the ultimate load of the system.

## Stress fields

The exact geometry of the fan borders is rarely required in practice. If necessary, a differential equation for these curves can be formulated with an equilibrium condition on a differential fan element.

The trajectory of the lower fan boundary AC is given by:  $z = \frac{f_c - q}{2qd(1 - \omega/2)} x^2$

The upper edge of the fan DF is also a second degree parabola.



### Fans and arches in beams without transverse reinforcement: exact fan geometry

The geometric trajectory of all (generally curved) elements of a stress field model can be determined analytically. This is shown in the following two slides for the boundary of the fan depicted above.

In practice, this accuracy is rarely required, since the basic dimensions can be determined with statically equivalent but simpler models.



## Stress fields

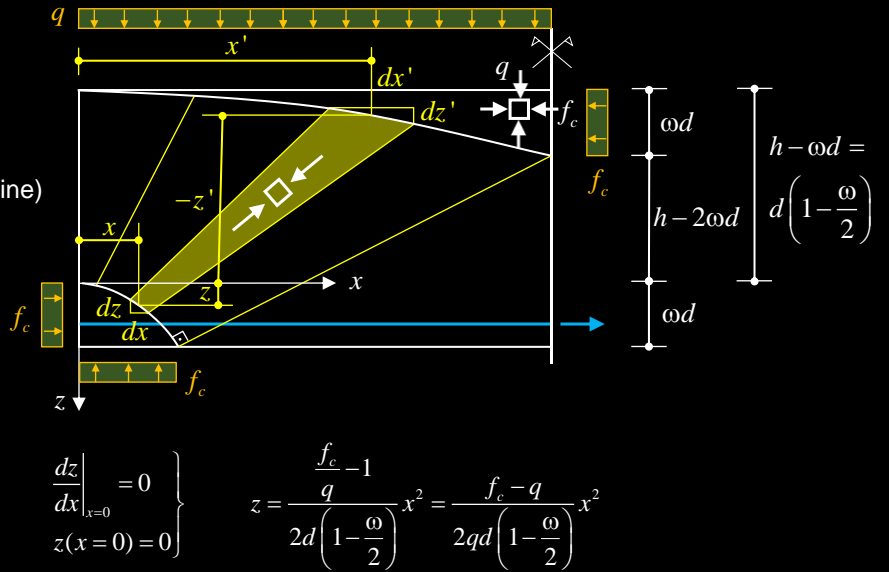
Equilibrium:

$$dx f_c = dx' q; \quad \frac{dx'}{dx} = \frac{f_c}{q}$$

$$dz f_c = dz' f_c \rightarrow (z - z') = \text{const. (affine)}$$

$$\frac{dz}{dx} = \frac{x' - x}{d \left(1 - \frac{\omega}{2}\right)}$$

$$\frac{d^2 z}{dx^2} = \frac{\frac{dx'}{dx} - 1}{d \left(1 - \frac{\omega}{2}\right)} = \frac{\frac{f_c}{q} - 1}{d \left(1 - \frac{\omega}{2}\right)}$$



**Fans and arches in beams without transverse reinforcement: exact fan geometry**

## Stress fields

### Load suspension mechanism

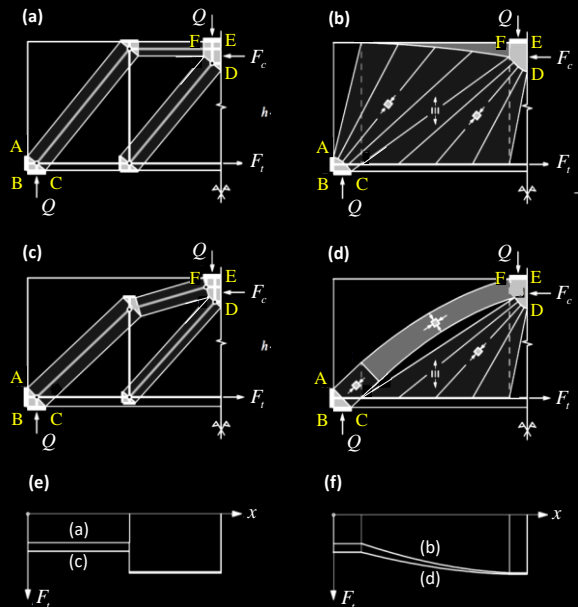
The **minimum amount of vertical reinforcement** (stirrups) can be **activated** by a load suspension mechanism. This reduces the tensile force to be anchored behind the support.

In all four models the bearing and the load introduction plates (B-C, E-F) are identical. Therefore, the lower bounds of the ultimate load are identical in all models as well.

The stress fields (right) can be derived from the simple strut-and-tie models (left).

The entire load can be suspended (upper models) or only a part of it (lower models).

The **distribution of the force in the tension chord** (lowest row) and the force to be anchored behind the support can be derived from the respective stress fields.



22.09.2021

ETH Zurich | Chair of Concrete Structures and Bridge Design | Advanced Structural Concrete

26

### Load suspension mechanism: beams with transverse reinforcement and point load

This slide introduces the concept of the load suspension mechanism in a beam with a point load. Instead of transferring the load directly to the support via compression elements, it can be partially or totally suspended by placing vertical reinforcement. This leads to a decrease of the force acting in the horizontal tension chord. The decrease can be either discrete, as in strut-and-tie models (a) and (c) (see *tension chord forces in (e)*), or continuous as in the stress fields shown in figures (b) and (d) (see *tension chord forces in (f)*). This makes it easier to anchor the force in the flexural reinforcement at the support. Moreover, in comparison with models without shear reinforcement, steeper and generally more favourable inclinations of the compressive field result (see influence of the effective compressive strength).

Similarly to the direct strut mechanism with distributed load, both a pure fan mechanism and a combined arch and fan mechanism can be assumed. The stress fields depicted in figures (b) and (d) can be derived from the strut-and-tie models shown in pictures (a) and (c), analogously to the case without shear reinforcement.

The load introduction and bearing plates have the same dimensions  $b = Q/(b_w f_c)$  in all four models, therefore, the same lower bound of the ultimate load is derived in the four equilibrium states.

## Stress fields

### Load suspension mechanism

#### (a,b): Load $Q$ totally suspended

- Larger amount of stirrups required, but smaller tensile force to be anchored
- Larger lever arm, therefore smaller  $F_c$  and  $F_t$  at midspan than in models (c, d)

#### (c,d): Load $Q$ partially suspended

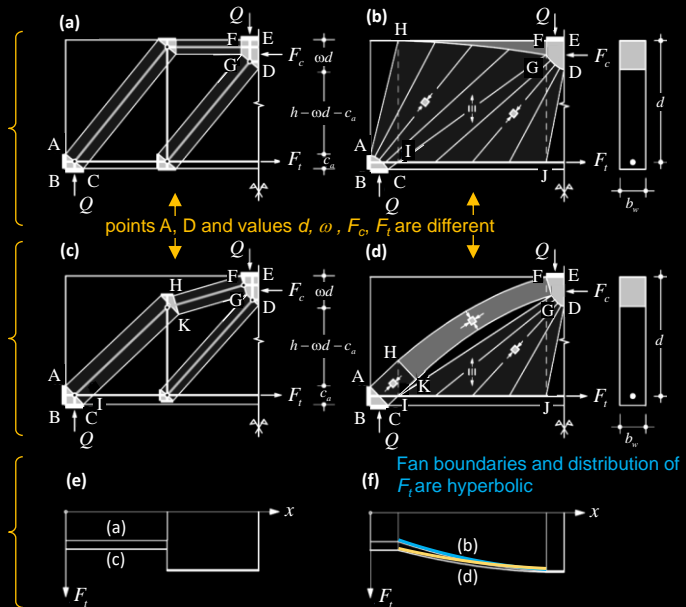
- Lower amount of stirrups required, but larger tensile force to be anchored
- Smaller lever arm (\*), thus larger  $F_c$  and  $F_t$  at midspan than in models (a, b)

(\* since distance AB is higher

#### Tension chord force distribution $F_t$

- (a,c) steeped, (b,d) continuous
- $F_{t0} = F_{t0} < F_{t0} = F_{t0}$  at midspan
- $F_t$  in all cases lower than with direct strut mechanism

RN3



22.09.2021

ETH Zurich | Chair of Concrete Structures and Bridge Design | Advanced Structural Concrete

27

## Load suspension mechanism: beams with transverse reinforcement and point load

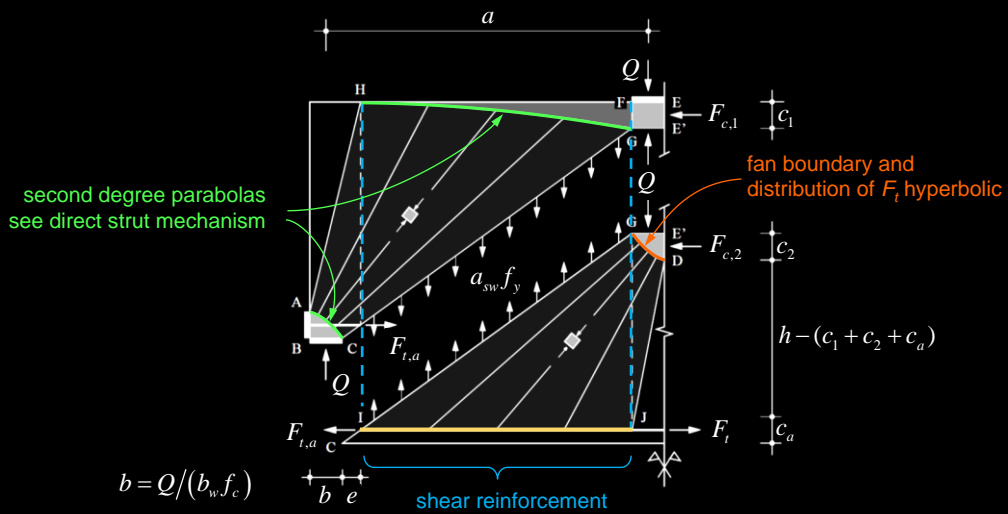
In stress field (b), the entire load  $Q$  is carried to the horizontal bending tie over the fan DGIJ. The load is suspended to the upper edge FH of the membrane element by means of the parallel vertical tension field FHIJ. The load is then transmitted to the edge GH by compression zone GFH, in order to be transmitted to the support through the fan ACGH.

In stress field (d), only part of the load  $Q$  is carried to the horizontal bending tie over the fan DGIJ and then suspended to the upper edge FH of the arch by means of the parallel vertical tension field FHIJ. The remaining part of  $Q$  is directly transmitted to the support by the arch GFHK and the strut ACKH. The combined arch and fan mechanism (d) requires less shear reinforcement than the fan mechanism alone (b), but the reinforcement force  $F_{tAB}$  to be anchored at the support and the height of the nodal zone ABC are greater. The effective height  $d$  is smaller and consequently the forces  $F_c$  and  $F_t$  acting at midspan are greater than for the fan mechanism alone (b). For the same reasons, the internal forces  $F_c$  and  $F_t$  at midspan of the membrane element of the stress fields (b) and (d) are smaller than for a direct strut mechanisms.

The distribution of the load between the arch and the fan mechanism in the stress field (d) can be freely chosen by the designer. If the load ratio carried by the arch is progressively increased, the curvature of the arch and the size of the fan DGIJ decrease gradually, while the length and width of the strut ACKH (which becomes flatter) increases. This way, the direct support mechanism is achieved as a limit case.

## Stress fields

### Load suspension mechanism (detail model b)



### Load suspension mechanism: beams with transverse reinforcement and point load

The fan ACGH in stress field (b) is analogous to the one of a direct strut mechanism for a distributed load. The fans DGIJ in stress fields (b) and (d) are supported at one end by a nodal zone and at the other by a straight reinforcement. The shape of the fan edge DG and the variation of the tension chord force are hyperbolic. The compressive stresses in the fan are  $\sigma_{c3} = -f_c$  at the node edge DG, and they decrease hyperbolically along the stress trajectories. Along the line IJ, the compressive stresses are in equilibrium with the vertical, uniformly distributed stirrup forces and with the horizontal bond-shear forces. The latter continuously reduce the force  $F_{t,i}$  acting in the tension chord.

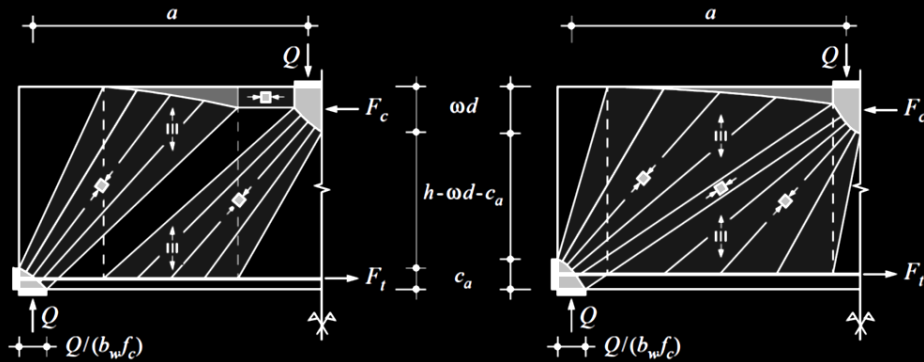
The stress field shows that only the shear reinforcement in the clear span (between the bearing plates) can be activated for the load suspension (strictly speaking, only in the area F-H or I-J). Stirrups over the bearing plates do not contribute to the suspension mechanism.

The exact geometry of the individual stress field elements can be determined exactly, but this is rarely necessary in practice. The distribution of the tension chord forces, particularly the forces to be anchored at the supports, can be determined from equilibrium considerations on appropriate equivalent models (statically equivalent strut-and-tie models are sufficient for determining the final anchorage force).

## Stress fields

### Load suspension mechanism: combination of basic models

Other possible stress fields (concentrated shear reinforcement, combined direct strut and suspension mechanisms suspension)



### Load suspension mechanism: beams with transverse reinforcement and point load

#### Other models by combination of basic models

The figure shows two stress fields related to the basic case of the pure fan mechanism on the last page. In the basic case, the area FHIJ with shear reinforcement was chosen wide enough so that the two fans share a border (i.e. have a common edge trajectory, GI). Alternatively, the distributed shear reinforcement can also be distributed over a shorter length, as shown in the stress field on the left.

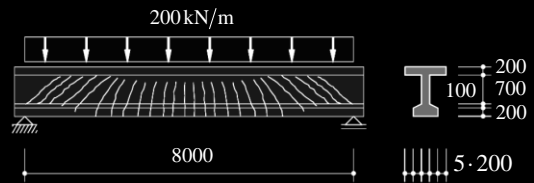
The stress field presented on the right shows a combined direct strut and suspension mechanism. Part of the load  $Q$  is transmitted directly to the bearing via a direct strut running between the two fans. Similarly to the case of the combined arch and fan mechanism, this requires less shear reinforcement than a pure fan mechanism. In return, the reinforcement force  $F_{tAB} = c_a b_w f_c$  to be anchored in the support as well as the forces  $F_c$  and  $F_t$  at midspan are greater.

## Stress fields

### Beam - Example 1 (see [4] p. 66 ff)

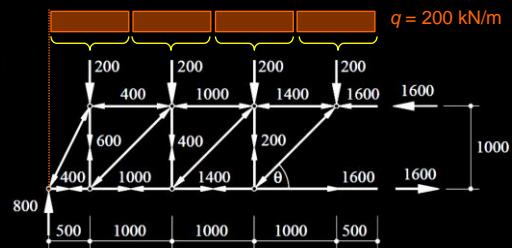
#### Beam with distributed load, expected crack pattern

- Idealization as a **plane element**
- **Upper/lower chord** reduced to the centre of gravity of the axes: "**Stringer**"
- **Web** modelled as **plane membrane element**



#### Possible strut-and-tie model

- Upper chord and struts (concrete) = compression forces
- Lower chord (longitudinal reinforcement) and vertical ties (stirrups) = tensile forces
- Distributed load reduced to statically equivalent individual loads in the nodes of the upper chord
- Correct geometry: nodes chosen in such a way that equivalent static nodal forces can be applied (thus the first compression diagonal is steeper!)
- If required, strut-and-tie models can be refined into stress fields



(forces in kN, dimensions in mm)

## Stress fields for beams

In the following, the basics of strut-and-tie models and stress fields for beams, which have already been presented in Stahlbeton I, are repeated.

From the discontinuous stress fields (strut-and-tie model), the required longitudinal and transverse reinforcement, as well as the constructive detailing, can directly be determined. The bending moment "offset" due to the interaction with shear is implicitly included. When defining the reinforcement, only the anchorage lengths have to additionally be taken into account, which is possible without special effort. It should be noted that the reinforcement should be distributed for those ties modelling e.g. the shear reinforcement. However, the ties modelling tension chords or concentrated ties should not be distributed.

The upper figure shows the load and the expected crack pattern of a simply supported double-T concrete beam. The beam is idealised as a flat element. The upper and lower chords are reduced to their centre of gravity (so-called "stringer") and the web is modelled as a flat membrane element.

## Stress fields

Beam - Example 1 (see [4] p. 66 ff)

Various possible strut-and-tie models

→ Different inclinations of the diagonal concrete struts

→ Flatter struts:

- more longitudinal reinforcement
- less shear reinforcement

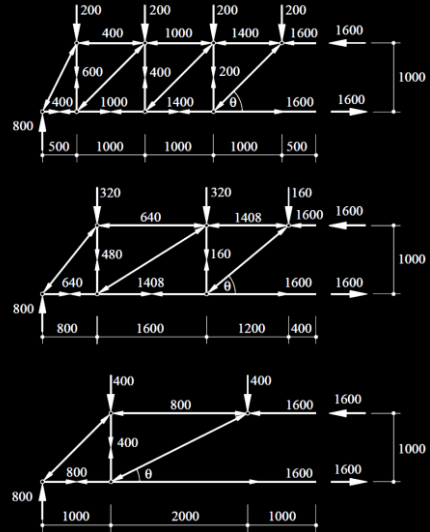
→ The influence of the inclination of the diagonal concrete compression field on the total reinforcement volume is low

**Note:**

→ Assessment of existing bridges designed according to earlier standards (inclined principal tensile stresses): The ultimate limit state verification is often only possible with very flat inclinations

→ Very flat inclinations lead to large vertical strains in the web → Concrete compressive strength is affected, brittle failure of stirrups can occur

→ SIA 262:  $k_c = \frac{1}{1,2 + 55\varepsilon_1} \leq 0,65$



The figures show alternative strut-and-tie models, based on different inclinations of the diagonal concrete struts. There are compressive forces in the upper chord and in the inclined diagonals (concrete struts) as well as tensile forces in the lower chord (longitudinal reinforcement) and in the vertical ties (shear reinforcement). The distributed load is reduced to statically equivalent single loads in the nodal zones of the upper chord. It can be seen that for flatter compression diagonals the required amount of longitudinal reinforcement increases and the required amount of shear reinforcement decreases.

The influence of the strain on the effective compressive strength of the concrete is detailed in the lecture notes on compatibility and deformation capacity.

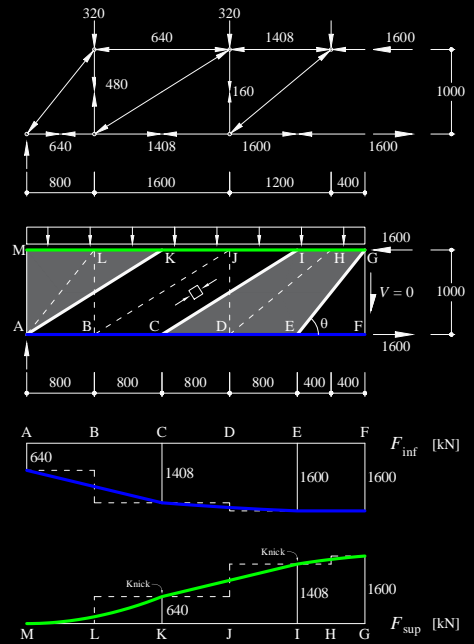
# Stress fields

## Beam - Example 1 (see [4] p. 66 ff)

### Strut-and-tie model and corresponding stress field

- Dashed lines = lines of action of the stress resultant of the individual elements of the stress field = struts and ties
- Resultants of the stress fields = values of the truss forces
- Tension and compression stringers AF and GM, fan CEGI, fan AKM centred at support point A, parallel compression tie ACIK, vertical ties CEIK and ACKM
- Determination of the chord forces = Stringer forces: **Equilibrium** of the load acting along the chord axes and the forces acting in the individual elements.
- Force distribution parabolic along fan edges CE, GI and KM, and linear along the edges of the parallel compression field (AC and IK)

- Vertical ties CEIK and ACKM: uniformly distributed forces (100 kN m<sup>-1</sup> and 300 kN m<sup>-1</sup> respectively)
- Chord forces from stress field and strut-and-tie model are identical in sections CK and EI (stirrup forces = discontinuity lines of the vertical ties)





## Stress fields

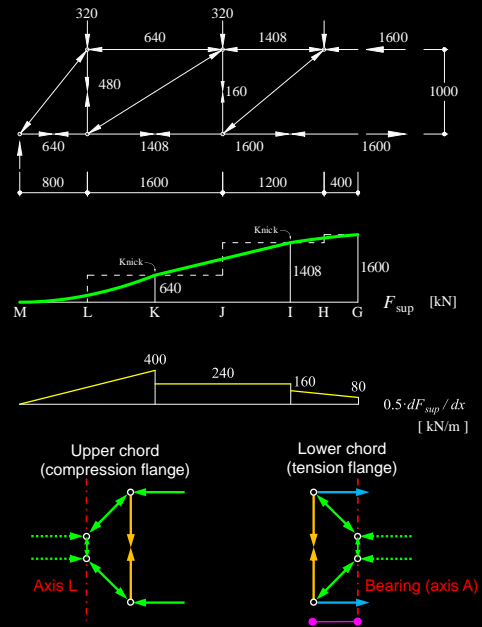
Beam - Example 1 (see [4] p. 66 ff)

### Propagation of the compressive force into the upper flange

- Simple 45° truss model (can be refined into a stress field)
- **Applied longitudinal force = Gradient of the longitudinal force in the compression stringer** = horizontal component of the compression forces in fans and parallel compression tie along GM
- The longitudinal force is supported by inclined struts on compression stringers (arranged in the centre of gravity axes of the upper flange).
- This results in **transverse tensile forces** → requires transversal reinforcement
- Consideration of web width = 200 mm in the strut-and-tie model = reduction of the transversal reinforcement of the upper flange

### Propagation of the tension chord force into the lower flange

- Analogous considerations (load is spread by means of transversal reinforcement to the longitudinal reinforcement bars distributed in the flange)
- Load spreading at the support A requires **extending the longitudinal reinforcement above the support** (in the order of half of the flange width to fully activate all tensile reinforcement)
- **Without extending the longitudinal reinforcement above the support** all the required tensile capacity (640 kN) at the support should be provided exclusively by the reinforcement below the web.



22.09.2021

ETH Zurich | Chair of Concrete Structures and Bridge Design | Advanced Structural Concrete

33

The two upper figures show the distribution of the compression stringer force.

A transversal stress results from the application of the shear force between the web and the flange. This shear force corresponds to the variation in the upper chord force, which (corresponding to  $dM/dx = V$ ) is directly related to the distribution of the transversal forces (horizontal component of the inclined struts in the stress field or strut-and-tie model).

The 45° transversal strut-and-tie model shown below illustrates the propagation of the compression stringer force into the upper chord. The introduced longitudinal forces correspond to the gradient of the longitudinal force in the compression stringer (or the horizontal component of the compression forces in the fans and in the parallel compression field along GM). It is in equilibrium with the compressive strings placed at the centre of gravity of the upper flange sides via inclined struts. This leads to transverse tensile forces, which require placing a transversal reinforcement in the flange. Note that the consideration of the web width in the strut-and-tie model reduces the required flange transversal reinforcement.

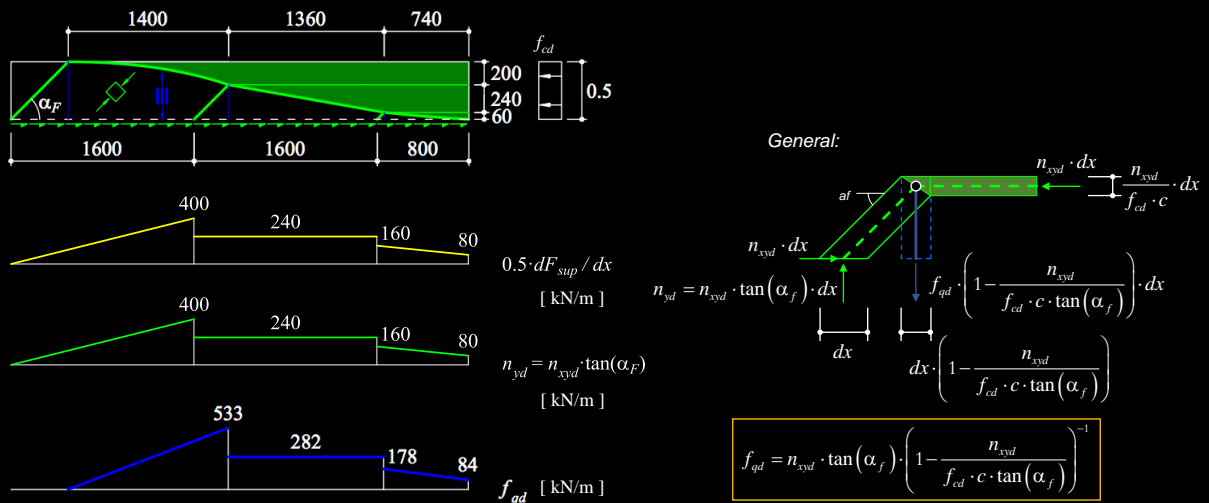
The tensile chord force should be distributed to the individual longitudinal reinforcement bars as well. The strut-and-tie models can be refined into equivalent stress fields for the spreading of chord forces.

### Additional remarks

To activate the entire flange width for bending (which is usually assumed in cross-section designs), the longitudinal force introduced by the web should be spread in the flange. A strut-and-tie model, which usually serves to determine the internal forces, is an idealization that does not allow capturing these effects. An "effective width" can be used to take into account the propagation under normal conditions. Based on this, the required transverse reinforcement can be determined.

## Stress fields - Transversal shear

Example – Top view of a T-beam



The concrete compressive strength  $f_{cd}$  is applied in the upper flange over the entire width at the section of maximum moment (bending capacity is reached; the effective flange width selected is accordingly). The shear forces, which are transferred from the web, are spread into the flange via a diagonal compressive stress field. The angle at which the compressive chord force is extended into the flange can be freely selected by means of the inclination of the compression field. However, it should be verified whether there is sufficient space for the compressive diagonals and for the distributed transversal reinforcement.

The compression chord force is spread in the flange, hence, a larger width of the flange is activated in compression in the middle of the T-beam than near-by the support. The width of the compression zone in the flange only corresponds to the "effective width" of the flange at midspan, and only in case this width could be activated at the selected angle of the spreading diagonal compressive field ( $\alpha_f$ ). Otherwise,  $\alpha_f$  should be increased if the entire effective width is to be used for the bending verification at midspan, what leads to a larger amount of transversal reinforcement in the flange.

### Additional remarks

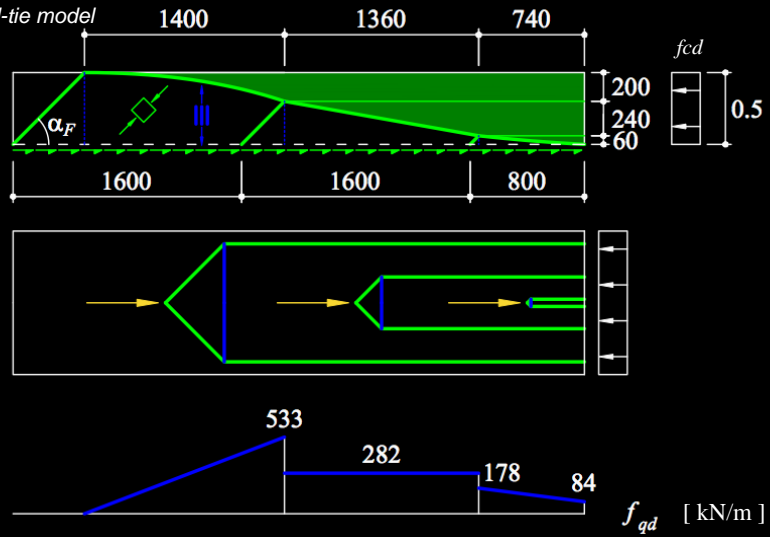
In practice, typically only the maximum transverse reinforcement is calculated and then inserted over the entire length (a maximum of 2-3 different amounts of reinforcement might be specified in certain cases).

The slide shows a stress field which does not require that the diagonal and the longitudinal compression fields cross each other. This results in relatively high transversal tensile forces (per m), since the transverse tensile reinforcement is only effective at a large distance from the support. Alternative stress fields in which the longitudinal force arriving close to the support is spread to a smaller width are also possible. This would allow activating the transversal reinforcement close to the support, resulting in lower transversal tensile forces (per m). However, the diagonal and longitudinal compression fields would intersect, making more difficult the verification of the compressive strength (if  $f_c$  is applied in the longitudinal direction, the compressive stress in the area of intersection would be  $> f_c$ ).

## Stress fields - Transversal shear

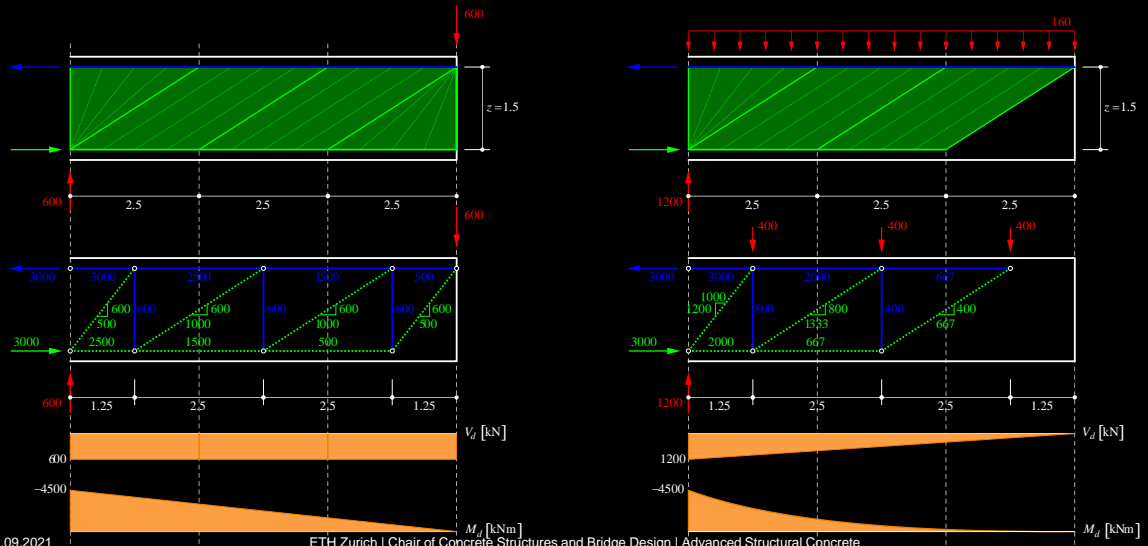
### Example – Top view of a T-beam

... and the associated strut-and-tie model



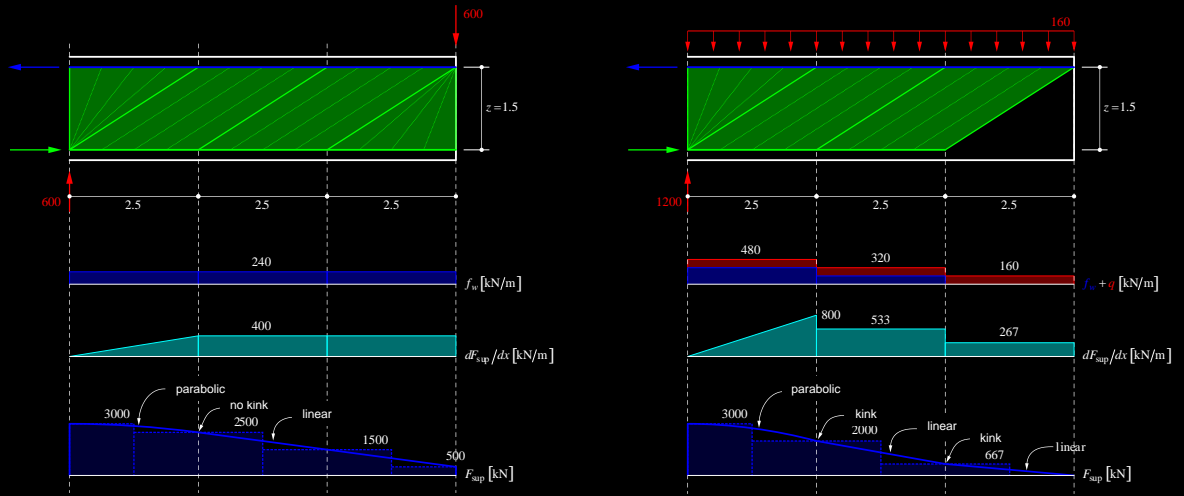
# Stress fields

Example 2: Cantilever beam with point and distributed load



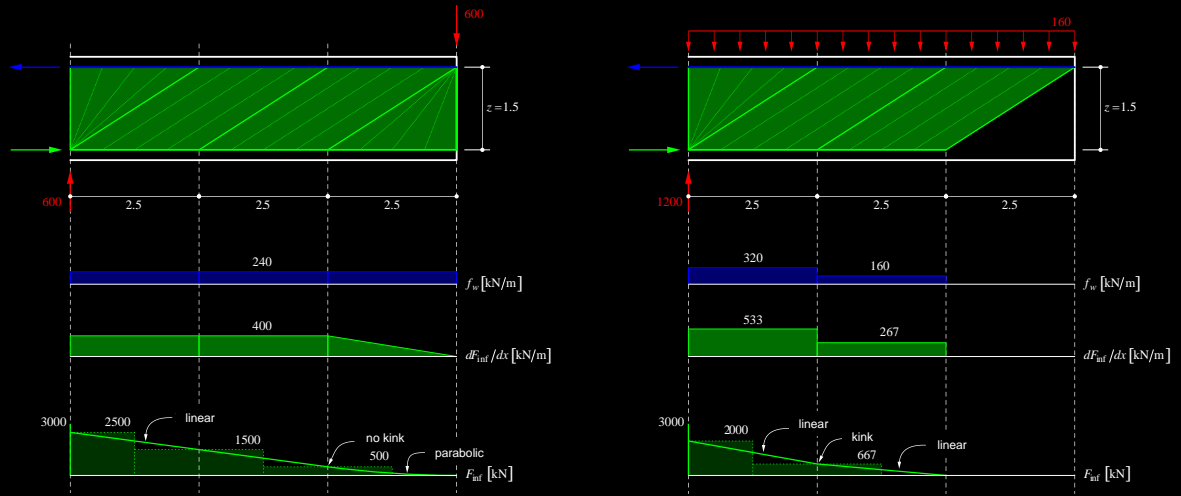
# Stress fields

Example 2: Cantilever beam with point and distributed load



# Stress fields

Example 2: Cantilever beam with point and distributed load



Additional examples can be found at the end of this document:

- Example 3: Combination of a simply supported beam with a cantilever
- Example 4: Beam with a variable depth

## Stress fields

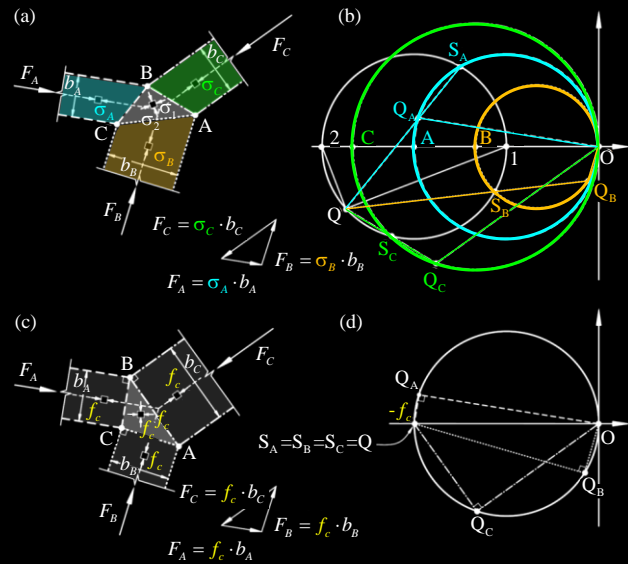
### Nodal zones

(a) General nodal zones: Struts with  $\sigma_A \neq \sigma_B \neq \sigma_C$   
(Forces in equilibrium!)

- Compressive stress in the nodal zones  $\sigma_2 < \min(\sigma_A, \sigma_B, \sigma_C)$ , except if node boundary  $\perp$  corresponding strut
- Connecting line of the poles of Mohr's circles of stress states on both sides of a discontinuity line // stress discontinuity line

(c) nodal zone with  $\sigma_A = \sigma_B = \sigma_C$  (relevant in practice)

- Node boundaries  $\perp$  struts, node geometry affine to polygon of strut forces (equilibrium)
- «Hydrostatic» stress condition  $\sigma_1 = \sigma_2 = f_c$  (strictly speaking not hydrostatic, as  $\sigma_3 = 0$ )



22.09.2021

ETH Zurich | Chair of Concrete Structures and Bridge Design | Advanced Structural Concrete

39

### Nodal zones

In the previous examples, the stress field models have been formulated. From the forces in the ties ( $F_t$ ), the reinforcement can be easily designed ( $A_s \geq F_t/f_{yd}$ ). **In the following slides it will be discussed how the concrete strength should be verified (both for nodal zones and fans).** Nodes where three or more ties join (often called as TTT nodes) should be avoided (other suitable stress field model should be proposed).

In figure (a), three struts with different stresses meet (this is often called a CCC node); the three forces are in equilibrium. The larger main compressive stress in the nodal zone is higher than the largest compressive stress in the struts unless the node boundary is perpendicular to the corresponding strut. The connecting line of the poles of the Mohr's circles on both sides of a discontinuity line is parallel to the stress discontinuity line, Figure (b).

The nodal zones shown in figures (c) (as well as (e) and (f) on the following page) have the same stress in all struts are much simpler and more useful in practice. The node boundaries are perpendicular to the struts and the node geometry is affine to the polygon of the strut forces.

In the nodal zones of the figures (c) as well as (e) and (f) on the following page, there is a biaxial uniform stress state  $\sigma_1 = \sigma_2 = f_c$  (often called "hydrostatic" for simplicity although the stress state is not hydrostatic, because the stress perpendicular to the membrane plane is  $\sigma_3 = 0$ )

## Stress fields

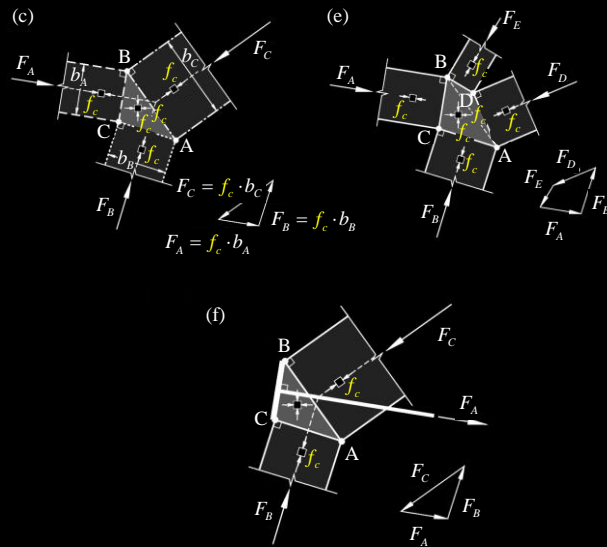
### Nodal zones

#### (e) Replacement of a strut (C) by two statically equivalent struts (D, E)

- Only the shape of the node boundary around the replaced strut changes, the remaining boundaries stay the same.
- Useful when considering fan stress fields (node dimensions based on the stress resultant = define node dimensions on a simple strut-and-tie model; exact shape of the boundary is usually not relevant)

#### (f) Treatment of tensile forces

- Anchored behind the nodal zone, treated like a compressive force (see constructive solutions in the next slide)



If the strut C in figure (c) is replaced by two statically equivalent struts D, E, only the shape of the node boundary around the replaced strut changes (figure (e)), the remaining boundaries stay the same (nodes A, B, and C are constant).

This is particularly useful when considering fan stress fields (node dimensions can be determined from the resultant of the fan stresses or from simple strut-and-tie models) as the exact shape of the boundary is usually not relevant.

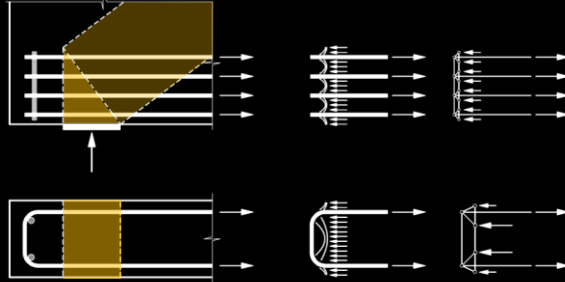
Tensile forces can be anchored behind the nodal zone by means of anchor plates that introduce a compressive force into the nodal zone. However, this is an unusual solution (see next page).



## Stress fields

**Nodal zones** (see [4] p. 64)

- **Proper constructive detailing is critical!**
- **Anchor plates** are not frequently used, but sometimes indispensable to anchor high tensile forces.
- Alternative i: **U-shaped links** see figures below. Local stress field → concrete cover can only be activated by the tensile strength of concrete
- Alternative ii: Use of **headed bars** ( $d \approx 3\emptyset$ ). Experimentally verified that the anchor length is very short ( $< 10\emptyset$ )  
→ Verification of the lateral spreading forces!
- Alternative iii: **Bent-up** flexural reinforcing bars (if enough space to develop a “compression banana” with deviation forces)
- Alternative iv: Stress fields with **continuous development** of bond shear stresses. Requires larger node dimensions.



22.09.2021

ETH Zurich | Chair of Concrete Structures and Bridge Design | Advanced Structural Concrete

41

### Nodal zones – detailing (repetition of Stahlbeton I)

The nodal zones must be treated very carefully in the process of design and detailing. Anchor plates are unusual in practice. However, they are sometimes the only way to anchor large tensile forces properly. Alternatively headed bars can be used.

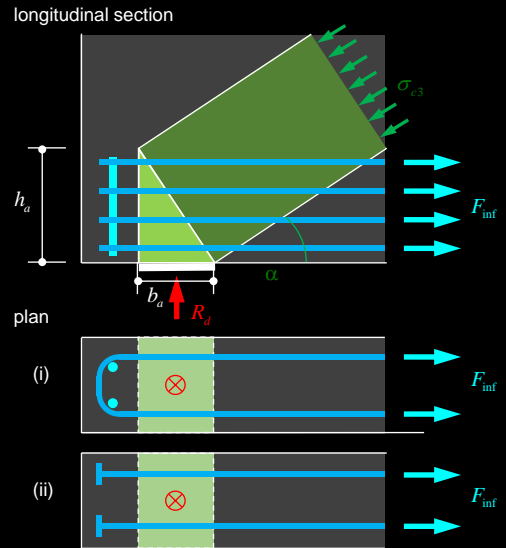
The figures on the left side show a possible detailing to anchor the main reinforcement by placing U-bars behind the nodal zone of an end support. The transfer of the distributed compressive stresses acting at the vertical edge of the nodal zone to the reinforcement (consisting of individual U-shaped bars) is ensured by compression fields between the concrete and the end loops of the bars. This load-bearing mechanism can be simulated with stress fields or strut-and-tie models, see figures on the right. It should be noted that concrete tensile stresses are required to ensure the load transfer from concrete to reinforcement. The transfer and distribution of the concrete compressive force to the reinforcement is improved by placing dowel bars at the end of the U-shaped bars.

Another alternative is to bend the main flexural reinforcement with sufficient anchorage length for the required tensile force to be anchored after the support (see page 33).

# Stress fields

## Nodal zones (see [4] p. 64)

- Proper constructive detailing is critical!
- Simplest solution: nodal zones with  $\sigma_h = \sigma_v$  (often referred to as "hydrostatic", but  $\sigma_1 = 0$ )
- Anchor plates are not frequently used, but sometimes indispensable to anchor high tensile forces.
- Alternative (i): Place U-shaped links, see pictures below. Local stress field  $\rightarrow$  concrete cover can only be activated by the tensile strength of concrete
- Alternative (ii): Headed bars (anchor plate diameter  $\approx 3\varnothing$ ), experimentally verified that the anchor length is very short ( $< 10\varnothing$ ). Verify the lateral spreading forces!



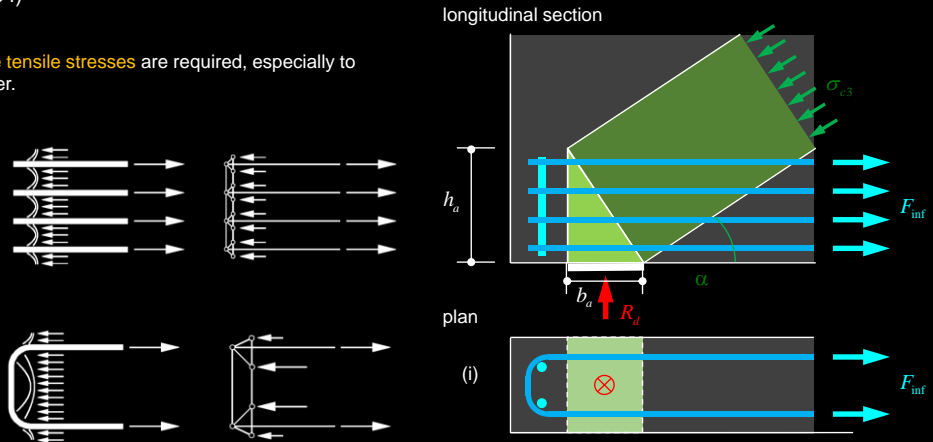
## Nodal zones – detailing (repetition of Stahlbeton I)

The nodal zones must be treated very carefully in the process of design and detailing. Anchor plates are unusual in practice. However, they are sometimes the only way to anchor large tensile forces properly. More frequent are the designs with reinforcement anchor elements presented above, such as (i) U-shaped links placed behind the nodal zone of the end support or (ii) headed bars.

## Stress fields

**Nodal zones** (see [4] p. 64)

- Strictly speaking **concrete tensile stresses** are required, especially to activate the concrete cover.



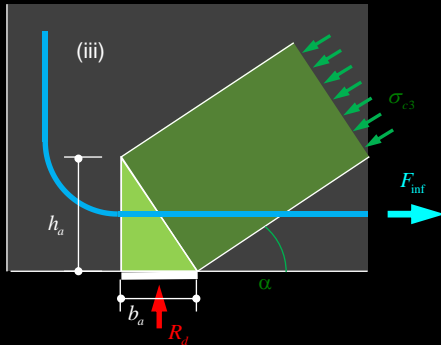
### Nodal zones – detailing (repetition of Stahlbeton I)

The transfer of the distributed compressive stresses (acting at the vertical edge of the nodal zone) to the reinforcement consisting of individual bars with end loops is realised by compression fields between concrete and the end loops of the bars. This load-bearing mechanism can be simulated with stress fields or strut-and-tie models, see figures on the left. It should be noted that concrete tensile stresses are necessary to ensure the transfer of forces from the concrete to the reinforcement. By placing dowel bars at the end of the U-shaped bars, the transfer and distribution of the concrete compressive force to the reinforcement is improved.

## Stress fields

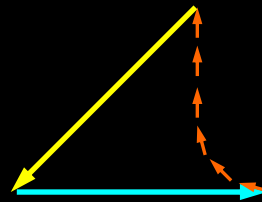
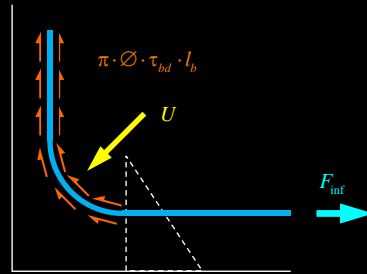
**Nodal zones** (see [4] p. 64)

longitudinal section

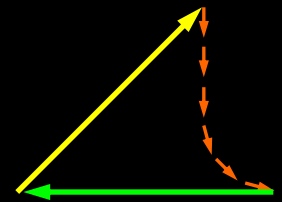
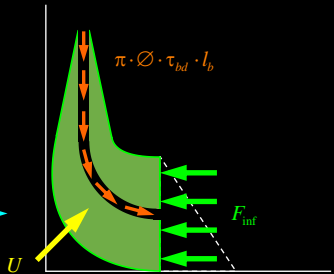


- Solution (iii): Bent-up reinforcing bars can be activated if there is sufficient anchorage length behind the support to anchor it ("compression banana" in the concrete with a deviation force  $U$ ).

reinforcement forces



concrete forces



22.09.2021

ETH Zurich | Chair of Concrete Structures and Bridge Design | Advanced Structural Concrete

44

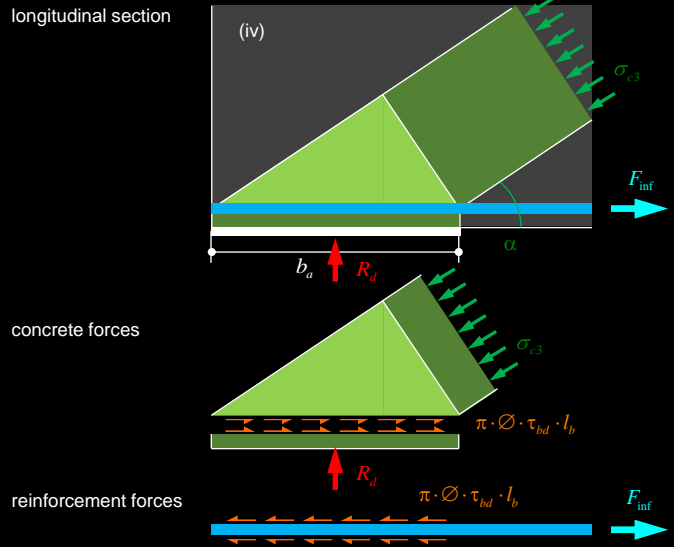
### Nodal zones – detailing (repetition of Stahlbeton I)

A frequently used alternative (iii) is to vertically bend up the flexural reinforcement with sufficient anchorage length. At the supports, at least 25% of the chord reinforcement required in the span shall be anchored (Section 5.5.2.5. SIA 262:2013).

## Stress fields

Nodal zones (see [4] p. 64)

- Alternative (iv): Stress field with **continuous development of tension chord force** through bond-shear stresses.
- Requires larger node dimensions (large anchorage length = node width, despite favorable effect of transverse compression on bond)



## Nodal zones – detailing (repetition of Stahlbeton I)

- Alternative (iv): Stress field with continuous development of tension chord force through bond-shear stresses.
- Requires larger node dimensions (anchorage length = node width, despite the fact, that the transverse compression has a favorable effect on bond)

## Stress fields

### Nodal zones (see [4] p. 64)

Disadvantages of solutions (i)-(iii) = "hydrostatic" nodal zone

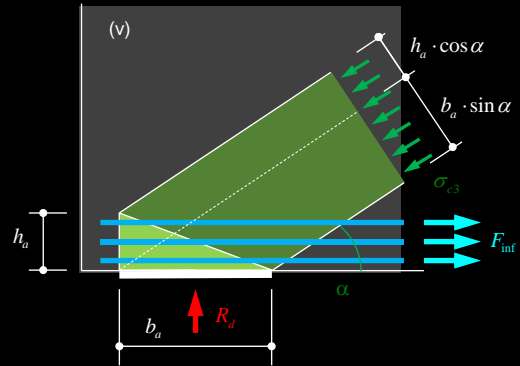
- Require a relatively large height of the nodal zone, which reduces the effective depth of the beam.
- Do not consider that a higher compressive strength may be applied in the nodal zone than in the strut (different values of  $k_c$ ).

Disadvantages of the solution (iv) = anchoring via bond-shear stresses

- Requires a large, often impracticable width of the nodal zone (= bearing plate)

Solution (v) (see, e.g. Canadian standard CSA)

- "free" choice of node height and width, leading to nodal zones with  $\sigma_h \neq \sigma_v$
- Compressive stress in strut < Compressive stress in nodal zone



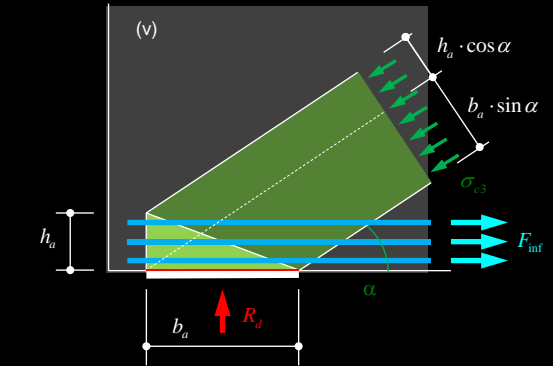
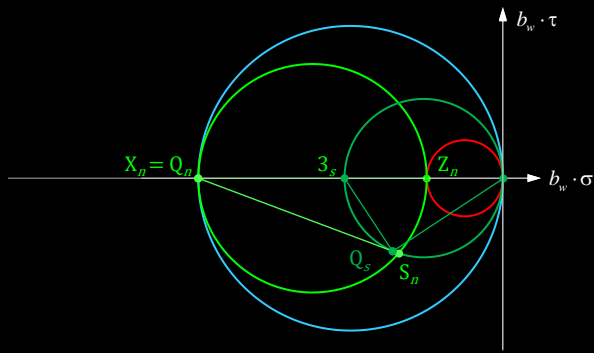
### Nodal zones – detailing

With the solution (v) the height and width of the support node can be freely selected. The stresses in the nodal zone are different horizontally and vertically, and the compressive stress in the strut has yet a different value.

# Stress fields

**Nodal zones** (see [4] p. 64)

Solution (v) (see Canadian standard CSA, among others): Stresses



- horizontal node boundary  $\sigma_v = -R_d / (b_a \cdot b_w)$
- vertical node boundary  $\sigma_h = -F_{inf} / (h_a \cdot b_w)$
- **N**: nodal zone ( $\sigma_v, \sigma_h =$  like node boundaries)
- **S**: strut  $-\sigma_{c3} = \frac{-R_d}{(b_a \cdot \sin \alpha + h_a \cdot \cos \alpha) \cdot b_w \cdot \sin \alpha}$

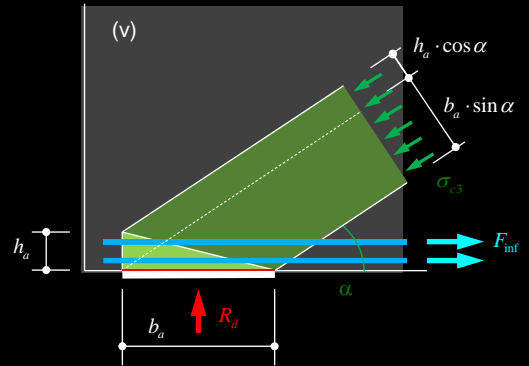
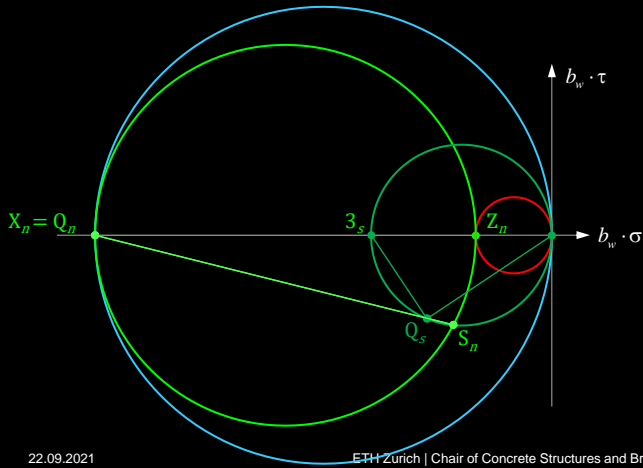
## Nodal zones – detailing

The stresses in the nodal zones and in the struts result from equilibrium.

# Stress fields

**Nodal zones** (see [4] p. 64)

Solution (v) (see Canadian standard CSA, among others): Stresses  
(Alternative with even smaller node height)



- horizontal node boundary  $\sigma_v = -R_d / (b_a \cdot b_w)$
- vertical node boundary  $\sigma_h = -F_{inf} / (h_a \cdot b_w)$
- **N**: nodal zone ( $\sigma_v, \sigma_h =$  like node boundaries)
- **S**: strut  $-\sigma_{c3} = \frac{-R_d}{(b_a \cdot \sin \alpha + h_a \cdot \cos \alpha) \cdot b_w \cdot \sin \alpha}$

22.09.2021

ETH Zurich | Chair of Concrete Structures and Bridge Design | Advanced Structural Concrete

48

## Nodal zones – detailing

In the case of small vertical dimensions of the nodal zone, the verification and detailing of the end anchorage should be examined very carefully (high horizontal stresses in the nodal zone are required!).



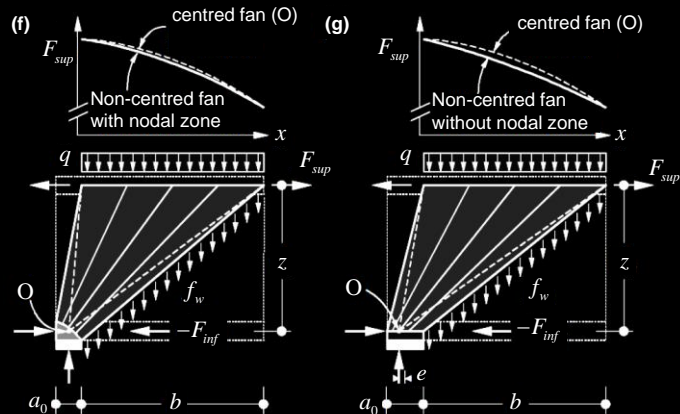
## Stress fields

**Concrete compressive stresses in fans: supports** (see [4] p. 70 ff)

→ (f) Usual solution:

**Non-centred fans with nodal zone**, see stress fields for membrane elements with rectangular cross section (in the nodal zone:  $-\sigma_{\text{cs}} < f_c \rightarrow$  define the dimensions of the bearing plate accordingly)

→ (g) Less suitable: **Non-centred fans without nodal zone** (requires longer length for the same  $f_c$ ; bond must be checked)



→ Chord force distribution  $F_{sup}$  in the fan area can be checked conservatively supposing a centred fan, provided that the height of the nodal zone according to (f) is in the flange (check with  $F_{inf}$  calculated assuming a centred fan). Otherwise the effective depth must be reduced (iteratively).

## Verification of compressive strength in fans: supports and point loads

Until now, we considered point-centred fans (in their corner the concrete compressive stresses are infinitely large). The required width of the bearing and load introduction plates cannot be verified using point-centered fans. Instead, non-centred fans can be used, see figure above (centred fans that do not converge at one point are not suitable, since a strong concentration of concrete compressive stresses occurs in the flattest trajectory, see next page). Fans with a nodal zone are useful in practice, left picture; fans without a nodal zone (right picture) result in excessively large bearing plates.

The shape of the node boundary results from equilibrium at a differential fan element. Usually it is sufficient to determine the height and width of the nodal zone; in this way, the fan can be replaced by the resulting strut, see above. The chord forces resulting from non-centred fans are lower than those from centred fans as long as the horizontal tensile force is not applied above the centre of gravity of the lower tension chord (in this case an iterative calculation with reduced effective depth is required). This means that the chord forces can be determined during design using the simpler centred fans.

## Stress fields

**Concrete compressive stresses in fans: fan instead of parallel field** (see [4] p. 70 ff)

→ (e) Not convenient: In centred fans with large changes of the inclination, the compressive stresses **at the bottom end of the flattest trajectory** are much bigger than in adjacent parallel compression fields, because the point with the flattest inclination, i.e. maximum  $(1 + \cot^2 \alpha)$ , and the largest stirrup force  $f_w$  coincide.

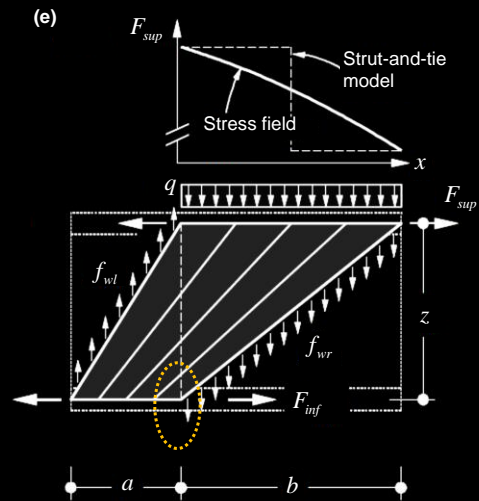
Note: In the adjacent parallel fields (for  $q = 0$ ):

$$-\sigma_{c3} = \frac{f_w (1 + \cot^2 \alpha)}{b_w}$$

$$f_w = \frac{V}{z \cot \alpha}$$

$$\rightarrow -\sigma_{c3} = \frac{V}{b_w z} (\tan \alpha + \cot \alpha) = \frac{V}{b_w z \sin \alpha \cos \alpha}$$

i.e. the flatter the diagonal compression field, the higher the stresses



### Verification of compressive strength in fans: distributed fan field

Instead of dividing the sections between points of zero shear force into equal sub-sections (which leads to fans only for concentrated loads or reactions and parallel compression fields for other cases), a stress field composed of several fans (see figure above) can be proposed. The stirrup forces on both sides of such fans are related by  $a \cdot f_{wl} = b \cdot (q + f_{wr})$ , and the compressive stresses  $-\sigma_{c3}$  in the web of the concrete are largest in the lower right corner of the fan (larger value of  $f_{wr}$  and flattest inclination, see above).

Strong changes in the inclination should be avoided, as the concrete compressive stresses are much bigger than in the adjacent parallel fields. This is illustrated on the following page for a specific case.

See also remarks on the effective concrete compressive strength in the following pages.

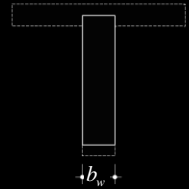
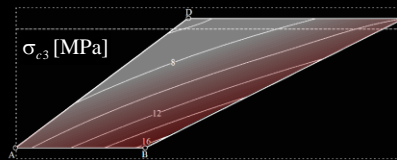
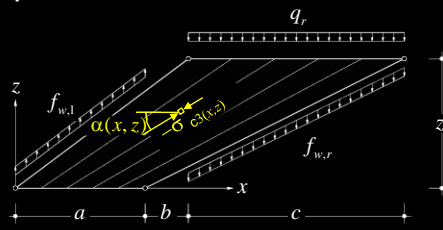
## Stress fields

### Concrete compressive stresses in fans: fan instead of parallel field

#### Numerical example

- Concrete compressive stresses vary significantly with small changes of  $\alpha$  (in adjacent parallel compression fields approx. 5 MPa to 10 MPa, but in point B 16 MPa!)
- Difference to nodal zones in supports: no transversal compression (vertical) due to the reaction and no transversal restraint (horizontal) due to the bearing plate or adjacent fans  
⇒ situation much worse

→ Strong changes of the inclinations are very unfavourable and should be avoided!



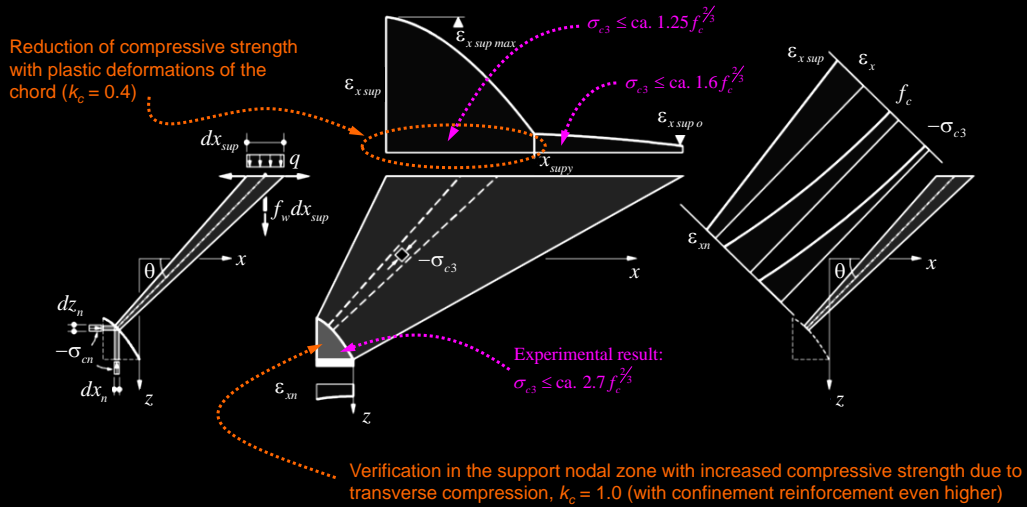
[from Marti and Stoffel 1999]

### Verification of compressive strength in fans: distributed fan field

The slide shows the results of a numerical analysis.

## Stress fields

### Concrete compressive stresses in fans: variable compressive strength



### Concrete compressive stresses in fans: variable compressive strength

The figure shows a general, non-centred fan over a support. In order to determine the web thickness (or to verify that the concrete compressive stresses are lower than the concrete compressive strength), the entire fan should be analyzed. Although the compressive stresses in the fan are greatest in the lower area (support), the compressive strength is lower in the upper area. This is caused by the different reduction factors of the compressive strength: the effective compressive strength is reduced by the (transverse) strains imposed by the upper tension chord, but increased by the transverse compression acting in the bearing area (see following page, determination of the effective concrete compressive strength). Thus it is not clear a priori which location is most restrictive.

The comparison of the hyperbolically varying compressive stresses in the fan along the trajectories with the corresponding compressive strength (shown schematically in the figure) shows that the failure occurs either along the upper tension chord (with large plastic chord strains) or in the nodal zone (highest stress). The fan area in between, is not critical. This can also be observed in experiments.

The verification of the concrete compressive strength and the selection of suitable factors to reduce the uniaxial compressive strength will be further discussed in '2.3 Walls and beams – Compatibility and deformation capacity'.

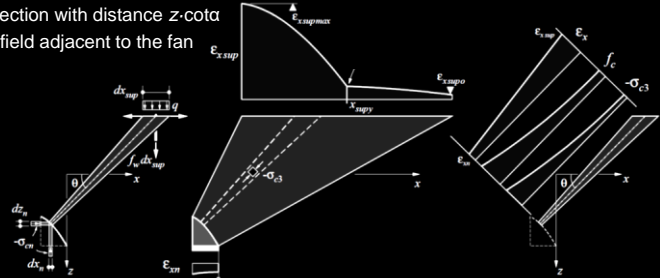
## Stress fields

### Concrete compressive stresses in fans

- Concrete compressive stresses vary hyperbolically along the trajectories
- Strain state also varies along the trajectories, which modifies the effective concrete compressive strength as well

$$\text{SIA 262: } k_c = \frac{1}{1,2 + 55\varepsilon_1} \leq 0,65 \quad \varepsilon_1 = \varepsilon_x + (\varepsilon_x + 0,002) \cot^2 a$$

- Verification of concrete compressive strength in a fan is complex
- Under normal conditions, no failure occurs in the fan as long as the tension chord reinforcement does not yield.
- Verify by checking the compressive stresses in the nodal zone (with increased strength due to transverse restraint or transverse compression) as well as in the parallel compression field adjacent to the fan (with yielding of the chord reinforcement in the area under consideration = incl. fans with reduced strength).
- SIA 262: Cross-sectional analysis = nominal verification in the section with distance  $z \cdot \cot a$  to the support, corresponds to a verification in the compression field adjacent to the fan
- Approximation without analysis of the strain state  $k_c = 0,55$ , when the tension chord reinforcement yields in the nodal zone: reduction of  $k_c = 0,4$



22.09.2021

ETH Zurich | Chair of Concrete Structures and Bridge Design | Advanced Structural Concrete

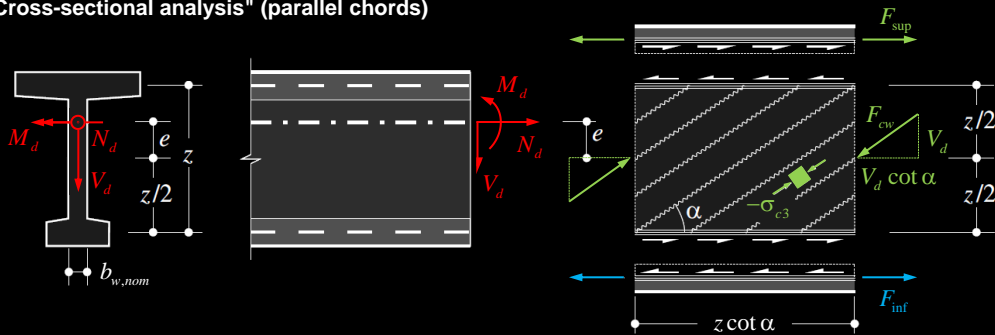
53

On the basis of the considerations presented on the previous page, the compressive strength verification in the web can be carried out as follows:

- Verification of the compressive strength over the support (with  $k_c = 1$  due to the existing biaxial compression).
- Check the compressive strength in the parallel compression field adjacent to the fan (according to SIA 262), with  $k_c = 0,55$  (no yielding of the tension chord reinforcement) or  $k_c = 0,4$  (yielding the tension chord reinforcement, in the case of plastic moment redistribution from the support).

## Stress fields

### Beam - "Cross-sectional analysis" (parallel chords)



- Dimensioning by "cross-sectional analysis" is possible, provided that all static and geometric values along the beam axis vary only gradually (not abruptly!).
- Internal forces ( $M, N$ ) should be related to the **centroidal axis**; for consideration of prestressing see haunched beams
- **Inclination of the concrete compressive field** theoretically freely chosen; restrictions to avoid premature ruptures of the stirrups or aggregate interlock (SIA 262: Normal case 30...45°)

$$F_{\text{sup}} = \frac{-M_d + N_d \cdot e}{z} + \frac{N_d}{2} + \frac{|V_d| \cdot \cot \alpha}{2}$$

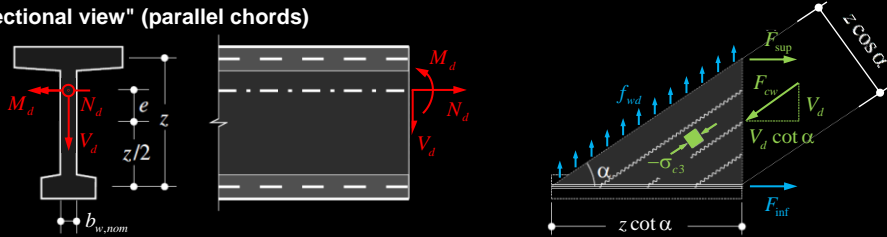
$$F_{\text{inf}} = \frac{M_d - N_d \cdot e}{z} + \frac{N_d}{2} + \frac{|V_d| \cdot \cot \alpha}{2}$$

Although a cross-sectional view is generally not sufficient to investigate the lateral force resistance, the structural safety can be investigated by means of suitable sectional diagrams. When the beam properties vary smoothly (no large individual loads, no supports, no changes in geometry, etc.), a simple, parallel compression field is a sufficiently accurate assumption.

The resulting relationships correspond to the load-bearing verifications of SIA 262.

# Stress fields

## Beam - "Cross-sectional view" (parallel chords)



- Equilibrium at the sectional member (upper right figure)

Force in the reinforcement  $f_{wd}$ :

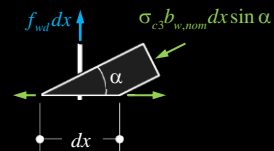
$$f_{wd} = |V_d| / (z \cot \alpha) \leq a_{sv} f_{sd}$$

- Equilibrium at the differential element (bottom right figure)

Concrete compressive stress  $\sigma_{c3}$  in the web:

$$-\sigma_{c3d} = |V_d| / (b_{w,nom} z) (\tan \alpha + \cot \alpha) \leq k_c f_{cd} \quad \text{mit} \quad b_{w,nom} = b_w - k_H \sum \varnothing_H$$

- Ducts in the web** disturb the compressive stress field → Reduce web width (see above), where  $k_H = 0.5$  (steel) or  $k_H = 0.8$  (plastic) applies for injected ducts,  $k_H = 1.2$  for non-injected ducts.
- Compressive stresses are minimal for **truss inclinations of 45°**; for flatter inclinations the stresses progressively increase and the concrete compressive strength decreases ( $k_c$ ).

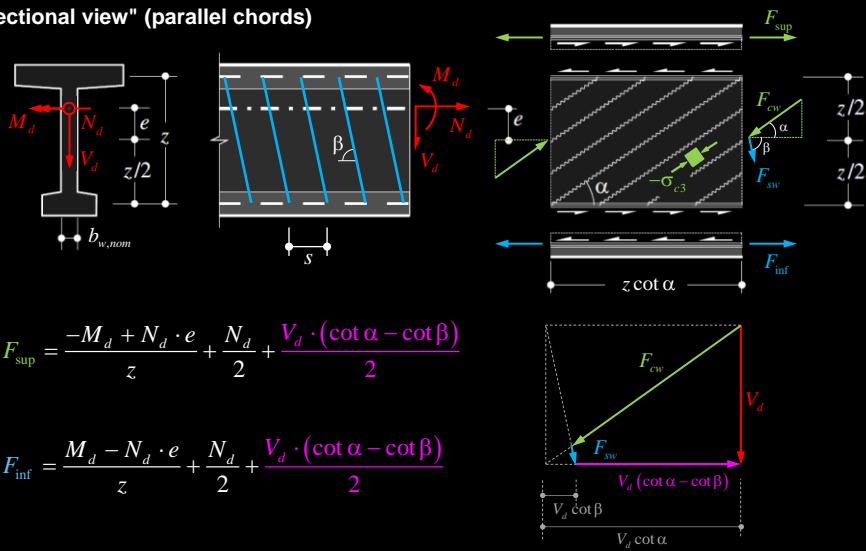


Note: Actually this is not a cross-sectional design, since stirrups are determined for a certain length ("staggering effect"); a cross-sectional design for shear force is strictly speaking not possible.

## Stress fields

Beam - "Cross-sectional view" (parallel chords)

Inclined stirrups



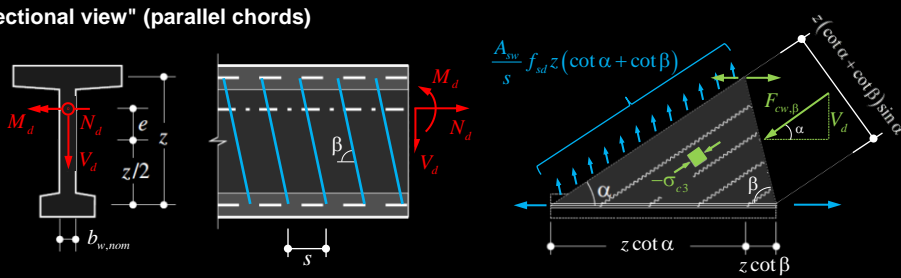
For inclined shear reinforcement, a "cross-sectional" verification is also possible.



## Stress fields

Beam - "Cross-sectional view" (parallel chords)

Inclined stirrups



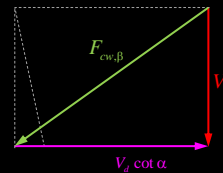
- Resistance of the shear reinforcement:

$$V_{Rd,s} = \frac{A_{sw}}{s} f_{sd} z (\cot \alpha + \cot \beta) \sin \beta \quad \left( = \frac{A_{sw}}{s} f_{sd} z \cot \alpha \right)$$

- Resistance of the concrete compression field:

$$V_{Rd,c} = b_w k_c f_{cd} z (\cot \alpha + \cot \beta) \sin^2 \alpha \quad (= b_w k_c f_{cd} z \sin \alpha \cos \alpha)$$

Vertical stirrups:  $\beta = \frac{\pi}{2}$

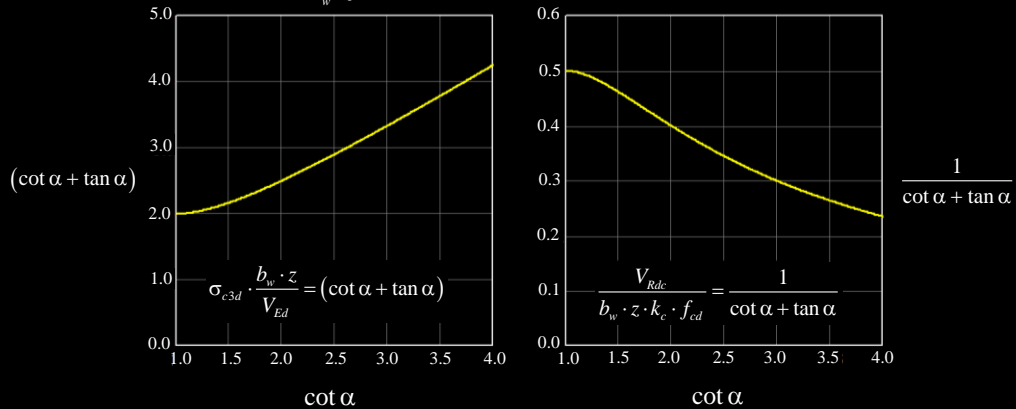


The shear resistance is limited by the capacity of the concrete  $V_{Rd,c}$  and by the capacity of the shear reinforcement  $V_{Rd,s}$ . The most restrictive value is decisive (not the sum, as in semi-empirical models). If inclined stirrups are provided (and if they are inclined in the correct direction!), the shear strength can be increased significantly for a given web width (for the same  $k_c$  by a maximum factor of 2).

## Stress fields

### Shear resistance depending on the compression field inclination (web concrete crushing failure)

$$\sigma_{c3d} = \frac{V_{Ed}}{b_w \cdot z} \cdot (\cot \alpha + \tan \alpha) \leq k_c f_{cd} \rightarrow V_{Rdc} = \frac{b_w \cdot z \cdot k_c \cdot f_{cd}}{\cot \alpha + \tan \alpha}$$



→ Concrete compressive stresses increase with flat inclinations

→ Dependence of the effective concrete strength depending on the inclination is not shown in these diagrams

### Shear resistance for constant $k_c f_{cd}$ (if the web compressive failure is decisive)

The graphs illustrate the distribution of the concrete compressive stress in the web (left side, proportional to  $(\cot \alpha + \tan \alpha)$ ) and the shear resistance in the case of a member where the compressive failure of the web is decisive (right side, inversely proportional to  $(\cot \alpha + \tan \alpha)$ ).

It can be seen that with flat compression fields (small angles  $\alpha$ ) greater concrete compressive stresses result, and the shear resistance decreases.

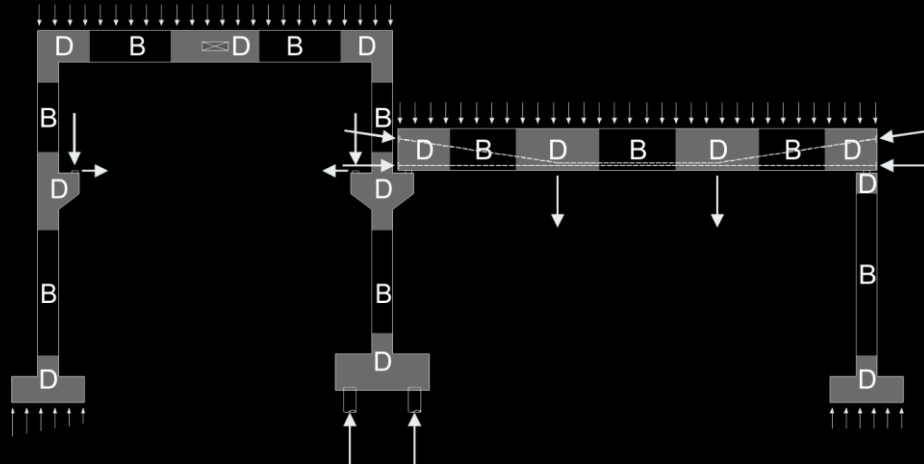
It should be noted that for  $\cot \alpha < 2.0$ ,  $k_c f_{cd} = 0.55 f_{cd}$  is typically considered, but for flat inclinations of the compression field ( $\cot \alpha > 2.0$ ) the compressive strength decreases. Therefore, the real reduction of the shear strength is even larger than what is shown in the figure (which assumes constant  $k_c f_{cd}$ ).

# Stress fields

Structural elements with static / geometric discontinuities

**B** Continuity/Bernoulli regions

**D** Discontinuity regions: static and/or geometric discontinuities



## Discontinuity regions

Cross-sectional design methods are only applicable to regions where the Bernoulli hypothesis (plane sections remain plain after deforming) is valid. However, in real-life structures large parts of the structures have static and/or geometric discontinuities. The stress field method is applicable for any kind of structure with or without static or geometric discontinuities.

# Stress fields

## Structural elements with static / geometric discontinuities

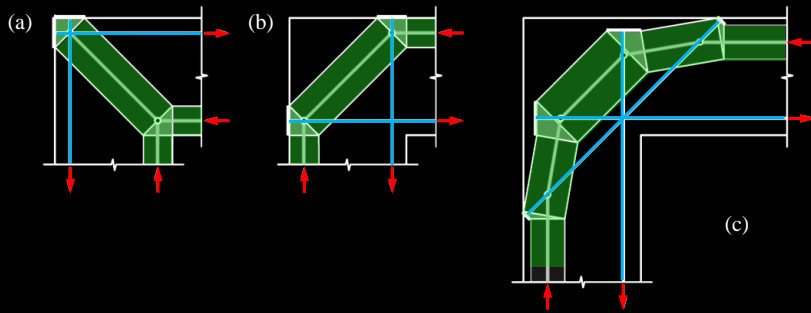
### Frame corners under pure bending

→ (a) Closing, (b) Opening moment

→ Especially opening frame corners are tricky and demanding in design

→ Diagonal reinforcement (c) is beneficial for anchoring the reinforcement forces

→ Bending resistance of the adjacent members usually cannot be fully exploited, since the anchoring and the deviation of forces in the corner area cause a reduction of the lever arm in comparison with (a), (b)



## Frame corners

Frame corners are a typical example of discontinuity regions, the design of which stress fields or strut-and-tie models are well suited for.

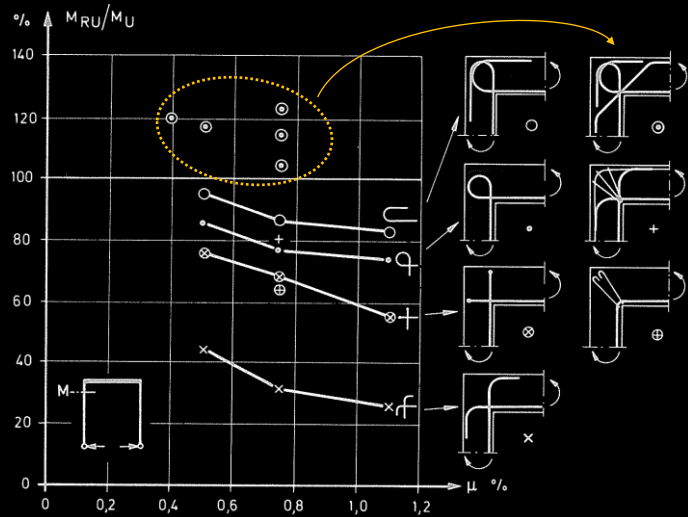
Relatively simple models are suitable for dimensioning, see figure. However, special attention should be paid to the anchorage of the reinforcing bars, see next page. Only with good detailing the full bending resistance of the connected beams or columns can be achieved, especially in case of high loads (and high reinforcement amounts). This is particularly important with opening frame corners (and any similar D-region, as e.g. dapped-ended beams, which will be discussed later), in which the CCT nodal zones differ very significantly from the typical CCT node over a support (in which the reinforcement is typically not at its maximum capacity and also can be fully anchored outside of the nodal zone). The difficulty of the anchorage of the reinforcement in CCT nodes is shown in the following by means of a series of experiments.

# Stress fields

## Structural elements with static / geometric discontinuities

### Frame corners under pure bending

- Experiments by Nilsson (1973) confirm the observations of previous slide
- Headed reinforcing bars are suitable in frame corners
- Examples of frame corners with distributed reinforcement, combined loading etc. see e.g. [5].



Tests on frame corners with opening moments show that even with sufficient anchorage length of the reinforcement, the full bending resistance of the connected transoms or supports cannot be achieved in all cases (tests by Nilsson in 1973, figures taken from Leonhardt).

In addition to the solutions shown in the figure above, anchorages with end plates also show good behaviour if the resulting spreading forces are covered with transverse reinforcement (missing in the figure, as this was unusual at the time).

## Stress fields

### Structural elements with static / geometric discontinuities

#### Dapped-end beams (d), (e), (f)

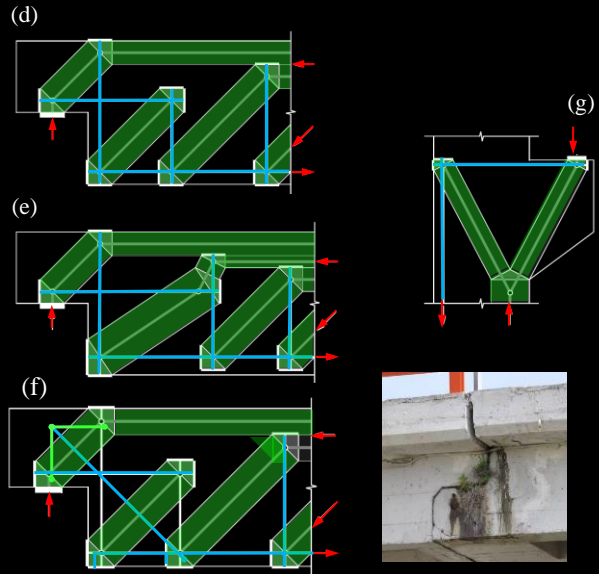
- (d), (e) possible strut-and-tie models
- Diagonal reinforcement favourable (f), analogously to the frame corners, superposition of the models (distribution of load can freely be chosen).
- Serviceability behaviour not covered by stress fields

#### Corbels (g)

- (f) Basic case
- Various other models possible, see e.g. [5]

#### General remarks

- Stress fields are perfectly suitable for structural elements with static or geometric discontinuities
- Figures only show simple strut-and-tie models
- Refinement through the introduction of fans, arches, tension and compression chords, etc. enables capturing the load-bearing mechanism of the concrete and the distributed reinforcement over the entire area (as will be shown in the following examples)



22.09.2021

ETH Zurich | Chair of Concrete Structures and Bridge Design | Advanced Structural Concrete

► Overpass road CV-500  
(Valencia, Spain)

62

## Dapped-end beams and corbels

In the past, dapped-end beams were very common, especially in Gerber joints (division of long bridges into sections, e.g. Hardbrücke Zurich). Because of pathologies caused by leaking transition joints (penetration of defrosting salts leads to corrosion, one of the causes of the collapse of the Viaduc de la Concorde in Canada in 2006), they are not allowed in swiss bridges any more.

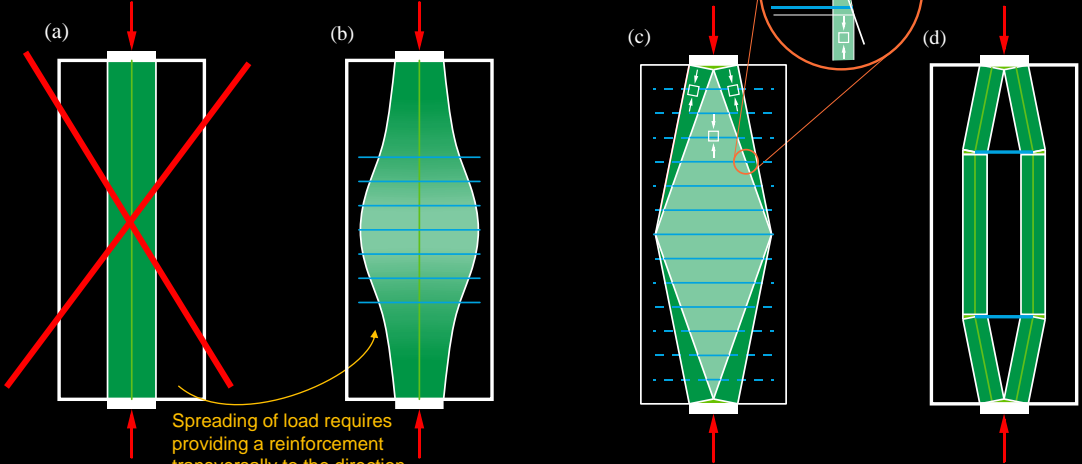
The behaviour is basically similar to that of frame corners and can be significantly improved with diagonal reinforcement. As recent tests and analytical investigations have shown (Mata Falcón, 2015), a suitable diagonal reinforcement can be used to control the crack width for the serviceability limit state (see next page).

Strut-and-tie models and stress fields are not suitable for investigating the serviceability limit state. In order to describe the actual behaviour, several possible strut-and-tie models should have to be superposed, whereby the load distribution would have to be found by using the minimum complementary energy (stiffest system). With approaches like the Compatibility-Based Stress Fields developed at ETH Zurich, such calculations can be performed automatically. It is basically a simplified, non-linear FE analysis including tension-stiffening (for more details see the chapter on numerical modelling).

# Stress fields

Structural elements with static / geometric discontinuities

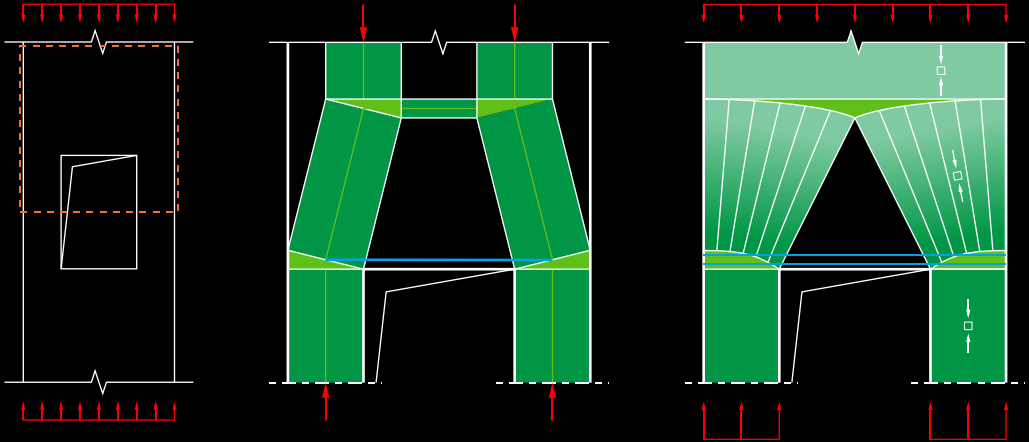
Spreading of concentrated loads in planar members



# Stress fields

Structural elements with static / geometric discontinuities

Wall with opening: further models can be built as combination or extrapolation of already known basic models





## Stress fields

### Comments for practical application («design»)

- In practical applications, the complete determination of the stress state in all components (fan edges, nodal zones, exact tension and chord force curves for fans ...) is not necessary.
- Suitable procedure in practice:
  1. Design the stress field roughly using scale drawings as combination of basic mechanisms (if necessary with simplifying assumptions such as centred fans and straight compression chords, see below)  
Most important basis: experience, understanding of the flow of forces, engineering judgement
  2. On this basis, determine sufficiently accurate chord force distributions, shear reinforcement and concrete compressive stresses at critical points.
  3. Determine important constructive details by designing the nodal zones
- Compression zones with variable height of the compression zone, which occur when the forces of the compression stringers cannot be spread into adjacent structural parts such as compression flanges (rectangular cross-sections), make the development of stress fields difficult.
- For the sake of simplicity, the compression zone can be reduced to a straight compression chord even in the absence of a compression flange, whose position (→ static height) should be determined conservatively in order to avoid insufficient concrete dimensions (theoretically correct: resultant of the corresponding part of the fan nodal zone).
- Serviceability behaviour cannot be verified.

### Remarks:

"Engineering judgement" is often nothing more than common sense (and experience). Of the points 1 to 3, point 3 is often the most important one to ensure a safe design.

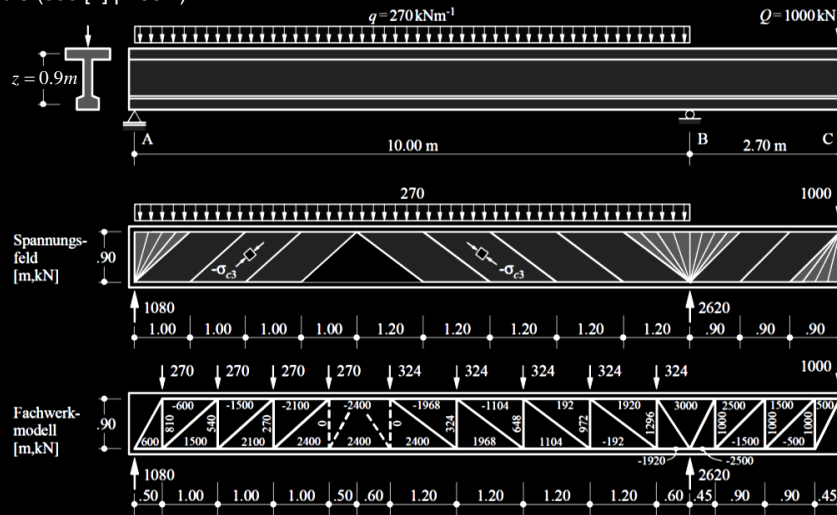
## Stress fields

### Comments for practical application («assessment»)

- Stress fields with combinations of load-bearing mechanisms (arcs and fans, struts and fans or orthogonal and diagonal reinforcement) are very difficult to assess. While they are of secondary importance for design purposes they might be necessary to assess existing structures and avoid unnecessary strengthening measures.
- The combination of load-bearing mechanisms can be easily analysed by means of Compatible Stress Fields (see numerical analysis chapter). This approach allows computing automating the most optimum stress field (i.e. the exact solution according to limit analysis) and accounts for all bearing mechanisms, including minimum reinforcement, whose strength contribution is typically neglected in stress fields.
- The Compatible Stress Field Method allows computing the serviceability behaviour (deflections, crack widths...), which is unknown in when using strut-and-tie models and stress field.
- Compatible Stress Fields are very suitable both for assessment and design purposes.

## Additional examples

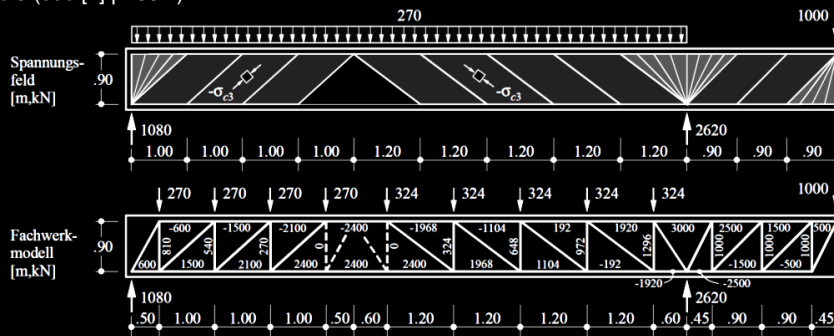
Beam - Example 3 (see [4] p. 66 ff)



The top figure shows a simply supported double-T reinforced concrete beam with a cantilever in one side and the applied loads. A suitable stress field, as well as the corresponding strut-and-tie model are shown below.

## Additional examples

Beam - Example 3 (see [4] p. 66 ff)



### Construction and elements of the stress field

- **Points of zero shear force** 4 m from support A, support B, beam end C
- Subdivision of the resulting sections into **equal sub-sections** → Inclinations of the parallel compression fields are  $\tan^{-1}(0.9/1.0) = 42.0^\circ$ ,  $\tan^{-1}(0.9/1.2) = 36.9^\circ$  and  $\tan^{-1}(0.9/0.9) = 45.0^\circ$ .
- **Centred fans** (compression trajectories intersect in one point) for concentrated loads
- **Tension chord, compression stringer and vertical ties** (shear reinforcement)

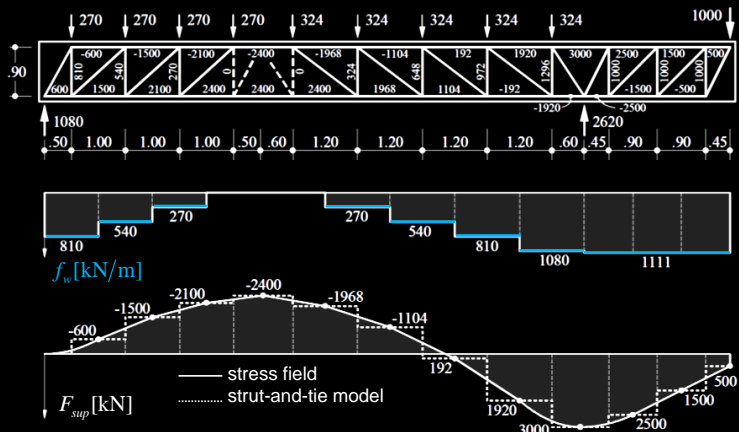
The shear force is zero at a distance of 4 m from support A, at support B and at beam end C. The different parts of the beams are subdivided into equally sized segments in order to define the strut-and-tie model. The stress field consists of (i) tension and compression stringers, (ii) fans centred at the points of introduction of concentrated forces, (iii) inclined parallel compression fields with side lengths of 1.0, 1.2 and 0.9 m (which corresponds to compression field inclinations of  $42.0^\circ$ ,  $36.9^\circ$  and  $45.0^\circ$ ) and (iv) vertical ties.

## Additional examples

### Beam - Example 3 (see [4] p. 66 ff)

#### Determination of forces in the stress field

- The stirrup forces  $f_w$  (per unit length) can be obtained directly from diagonal cuts at the boundaries of the parallel compression fields or fans; the forces are constant between two boundaries.
- The forces on the stirrups are constant in certain sections; as the load is applied at the top, the product  $f_w \cdot z \cdot \cot \alpha$  is inscribed in the shear force diagram (so-called "staggering effect")



- Load  $q_{int}$  applied below the upper chord should be suspended by the vertical reinforcement,  $\Delta f_w = q_{int}$
- Chord forces of the stress field and strut-and-tie model coincide at points (points with numerical values).

The distribution of the stirrup forces, shown in blue in the middle figure, is identical for the truss model and the stress field. As long as the loads are only applied on the upper chord and the girder is assumed to be weightless, the graded distribution is inscribed in the transversal force (staggering effect). It should also be noted that the stirrup forces can be determined directly from sectional diagrams with sections along the edges of the parallel compression fields or fans.

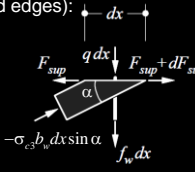
Any loads acting below the upper flange (in this case the insignificant weight of the web and the lower flange) must be suspended by means of additional shear reinforcement.

## Additional examples

Beam - Example 3 (see [4] p. 66 ff)

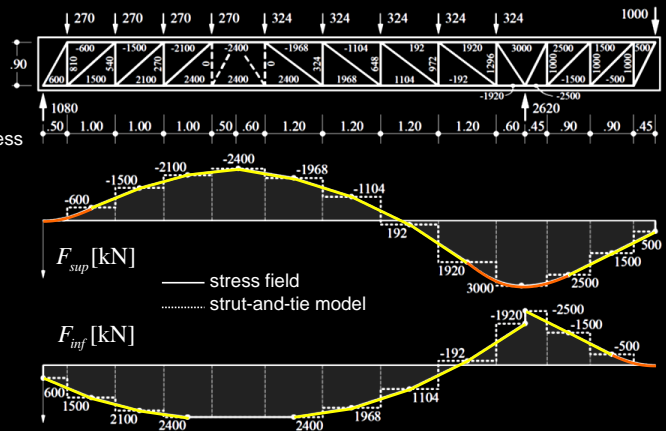
Determination of forces in the stress field

→ Distribution of chord forces  $F_{sup}$ ,  $F_{inf}$  and concrete compr. stress (chord edges):



$$-\sigma_{c3} = \frac{(q + f_w)(1 + \cot^2 \alpha)}{b_w} = \frac{q + f_w}{b_w \sin^2 \alpha}$$

$$\frac{dF_{sup}}{dx} = -(q + f_w) \cot \alpha \quad \frac{dF_{inf}}{dx} = f_w \cot \alpha$$



→ For a constant applied load  $q$ , the chord forces  $F_{sup}$ ,  $F_{inf}$  along parallel compression fields are linear ( $f_w$  and  $\cot \alpha$  constant), along centred fans are parabolic ( $f_w$  constant,  $\cot \alpha$  linear).

→ Concrete compressive stresses are constant in parallel compression fields (along stress trajectories and across the width of the compression field band), they vary hyperbolically along (straight) trajectories of the fans.

The figure shows the distribution of the longitudinal forces in the chords. As already mentioned, the chord forces of the stress field and the strut-and-tie model coincide at points where the vertical stirrup forces have a discontinuity.

In a parallel compression field the distribution of the chord forces is linear, but in the trajectory of a point-centred fan it is parabolic.

It should be noted that the concrete compressive stresses in the peaks of the point-centred fans are theoretically infinitely large.

## Additional examples

### Practical application - Example 4



22.09.2021

ETH Zurich | Chair of Concrete Structures and Bridge Design | Advanced Structural Concrete

71

Stress fields are of course also suitable for the design of prestressed bridges with variable cross section. An example design by Walter Kaufmann is the Vulpera Inn bridge, opened on 10.10.2010.

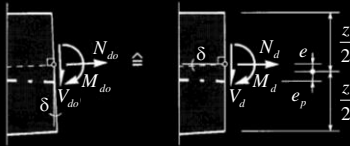
Additional remarks (see lectures on bridge design):

- The slenderness of the girder on cantilever bridges is usually approx.  $L/17$  above the piers and  $L/50$  at midspan (although a slightly higher depth is often provided to ensure accessibility).
- It is important to ensure that the lower flange is thick enough at the supports in order to absorb the total bending force; if the lower part of the web is in the compression zone (which is the case in some older cantilever bridges), this will be problematic: Not only the bending strength, but also the shear capacity is affected by the reduction of the lever arm in the internal forces.
- Some older cantilever bridges showed large long-term deformations which do not seem to decrease (as expected for creep deformations). These are usually bridges with too little prestressing; the most critical problems have appeared in bridges with a «joint» at midspan and thus a lack of continuity in the prestress. Too thin lower flanges above the supports are also unfavorable in this respect. Such problems can be avoided with a sufficient prestressing (and also continuous), which fully compensates the deformations due to permanent loads (taking into account friction and long-term losses).

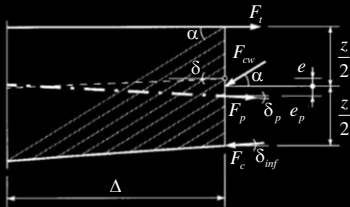
## Additional examples

### Practical application - Example 4

Beam - "cross-sectional analysis" (haunched beams with inclined prestressing)



$$\begin{aligned} N_d &= N_{do} \cos \delta + V_{do} \sin \delta \\ V_d &= -N_{do} \sin \delta + V_{do} \cos \delta \\ M_d &= M_{do} \end{aligned}$$



$$\begin{aligned} N_d &= F_i - F_{cw} \cos \alpha + F_p \cos \delta_p - F_c \cos \delta_{mf} \\ V_d &= F_{cw} \sin \alpha + F_p \sin \delta_p + F_c \sin \delta_{mf} \\ M_d &= F_i (z/2 - e) + F_{cw} \cos \alpha \cdot e - F_p \cos \delta_p (e_p + e) + \dots \\ &\quad \dots F_c \cos \delta_{mf} (z/2 + e) \end{aligned}$$

- Step 1: Translate the resultants from the beam statics calculation ( $M_{do}$ ,  $N_{do}$ ,  $V_{do}$ ) into the reference system of the stress field ( $M_d$ ,  $N_d$ ,  $V_d$ )
- Step 2: Formulate equilibrium on a vertical cut

By formulating equilibrium on suitable sectional diagrams and resolving the relationships for the desired variables, suitable information can be obtained for designing the chord and the shear reinforcement as well as for checking the web dimensions (concrete compressive stress).

In a first step (upper figures), the internal forces from the structural analysis (which apply to sections perpendicular to the beam axis, which is assumed to run in the centre of gravity of the beam) are converted into forces at a vertical section as shown in the upper figure.

The equilibrium is then formulated in this section, taking into account the chord inclination and the inclined prestressing force (which is applied as a force on the load side - usually without any increase in the prestressing force).

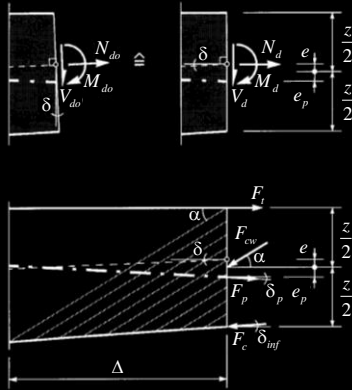
The force in the upper flange (cantilever construction, therefore continuous force during construction) is mostly absorbed by the cantilever prestressing; this is applied here as part of the tension chord force to be determined (i.e. on the resistance side). Alternatively, it could be introduced as a force in the formulation of equilibrium conditions, like inclined prestressing, which would further complicate the relationships.



## Additional examples

### Practical application - Example 4

Beam - "cross-sectional analysis" (haunched beams with inclined prestressing)



$$F_{cw} = \frac{2(V_d - F_p \sin \delta_p) - \tan \delta_{inf} \left[ 2 \frac{M_d}{z} - N_d \left( 1 - \frac{2e}{z} \right) + F_p \cos \delta_p \left( 1 + \frac{2e_p}{z} \right) \right]}{(1+k) \sin \alpha}$$

and

$$F_t = \frac{2k \frac{M_d}{z} + N_d \left( 1 + \frac{2ke}{z} \right) + \frac{V_d - F_p \sin \delta_p}{\tan \alpha} - F_p \cos \delta_p \left( 1 - \frac{2ke_p}{z} \right)}{1+k}$$

and

$$F_c = \frac{2 \frac{M_d}{z} - N_d \left( 1 - \frac{2e}{z} \right) - \frac{V_d - F_p \sin \delta_p}{\tan \alpha} + F_p \cos \delta_p \left( 1 + \frac{2e_p}{z} \right)}{(1+k) \cos \delta_{inf}}$$

with

$$k = 1 - \frac{\tan \delta_{inf}}{\tan \alpha}$$

→ Step 3: Determination of the stresses in the stress field and dimensioning of the elements

→ Source: Marti, P. "Shear design of variable-depth girders with inclined prestressing", Pre-stressed concrete in Switzerland, FIP Swiss Group, Zurich 1994, pp. 16-19

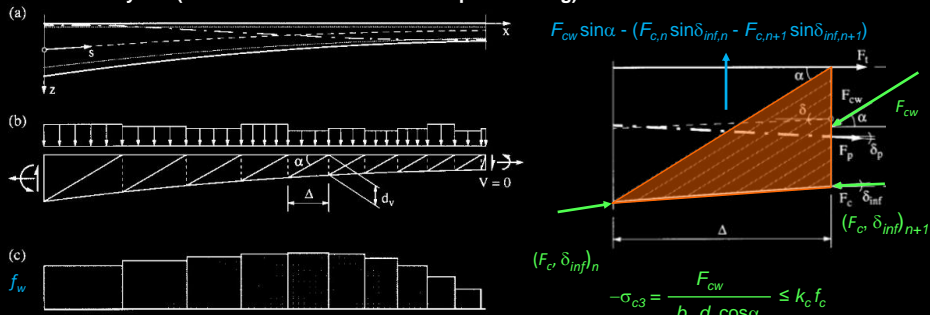
The obtained relations are generally valid for haunched (variable cross-section) beams with vertical stirrups and inclined tendons (see Marti, P., "Shear design of variable-depth girders with inclined prestressing", Pre-stressed concrete in Switzerland, FIP Swiss Group, Zurich 1994, pp. 16-19).

Since the longitudinal slope at the Vulpera Inn bridge was large (7.5%), the relationships were extended accordingly. The influence proved to be small; more important is the choice of whether the stirrups are arranged vertically or perpendicular to the upper slab.

## Additional examples

### Practical application - Example 4

#### Beam - "cross-sectional analysis" (haunched beams with inclined prestressing)



- The stirrup forces result from equilibrium at the shown cross sections (a bit smaller than  $F_{cw} \sin \alpha$ , favourable effect of the deviation forces of the curved lower chord).
- The deviation forces of curved tendons make the stirrup force variable over the web height, but this can usually be neglected.
- Verification of the concrete compressive stress or determination of the web width with the specified relation
- The distribution of the stirrup forces and concrete stress in the web can be controlled by the geometry of the lower chord («correct geometry»: this leads to the most uniform possible stresses over the entire length).

22.09.2021

ETH Zurich | Chair of Concrete Structures and Bridge Design | Advanced Structural Concrete

74

The forces in the vertical section determined following the indications of the previous slide can also be used to determine the web load (stirrup forces per metre, principal compressive stress). Due to the curvature of the lower chord, the stirrup forces are smaller than for a linear chord.

If the formulas are implemented in a computer program (or even a spreadsheet), the distribution of the internal forces over the beam length for different geometries of the beam can be easily investigated. Usually, the aim is to ensure that the stress on the stirrups is as constant as possible so that they do not have to be graded too much. For parabolic shapes of the lower chord (with their upper point at midspan) this requirement can be generally achieved with an exponent of slightly less than 2.

## Additional examples

### Practical application - Example 4



22.09.2021

ETH Zurich | Chair of Concrete Structures and Bridge Design | Advanced Structural Concrete

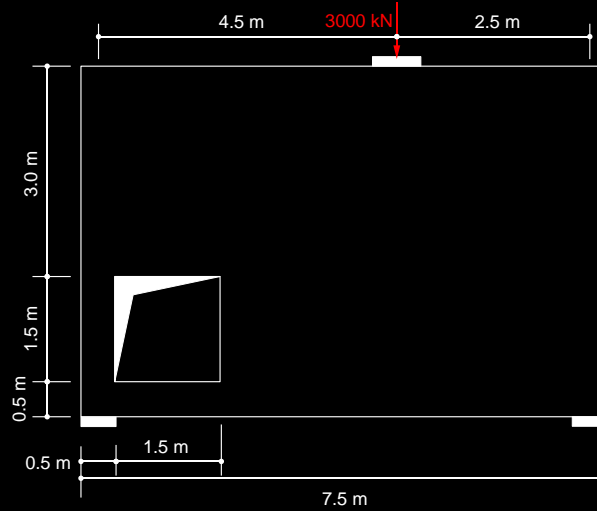
75

Vulpera Inn bridge : Impressions from the construction site.

## Strut-and-tie model – in-class exercise

### In-class exercise:

Discuss possible strut-and-tie models for the following example in Zoom break-out rooms



## Strut-and-tie model – in-class exercise

### In-class exercise:

Discuss which strut-and-tie models are **NOT** correct?

